

UNCLASSIFIED

AD NUMBER

ADB007945

LIMITATION CHANGES

TO:

Approved for public release; distribution is unlimited.

FROM:

Distribution authorized to U.S. Gov't. agencies only; Proprietary Information; SEP 1975. Other requests shall be referred to Rome Air Development Center, Griffiss AFB, NY.

AUTHORITY

RADC ltr 11 Mar 1982

THIS PAGE IS UNCLASSIFIED

**Best Available
Copy
for all Pictures**

AD B007945

AUTHORITY: RADC. USAF
TR, 11, MAR 82



AD B 007945

RADC-TR-75-247
Final Technical Report
September 1975



DEVELOPMENT OF ENCLOSED WIRE INTRUSION DETECTION TRANSDUCER

Westinghouse Electric Corporation, Hunt Valley, md

409513

Distribution limited to U. S. Gov't agencies only;
proprietary information; September 1975. Other
requests for this document must be referred to
RADC (OCDS), Griffiss AFB NY 13441.

AD No.
DDC FILE COPY

Rome Air Development Center
Air Force Systems Command
Griffiss Air Force Base, New York 13441

DDC
RECEIVED
DEC 10 1975
RECEIVED

A

UNCLASSIFIED

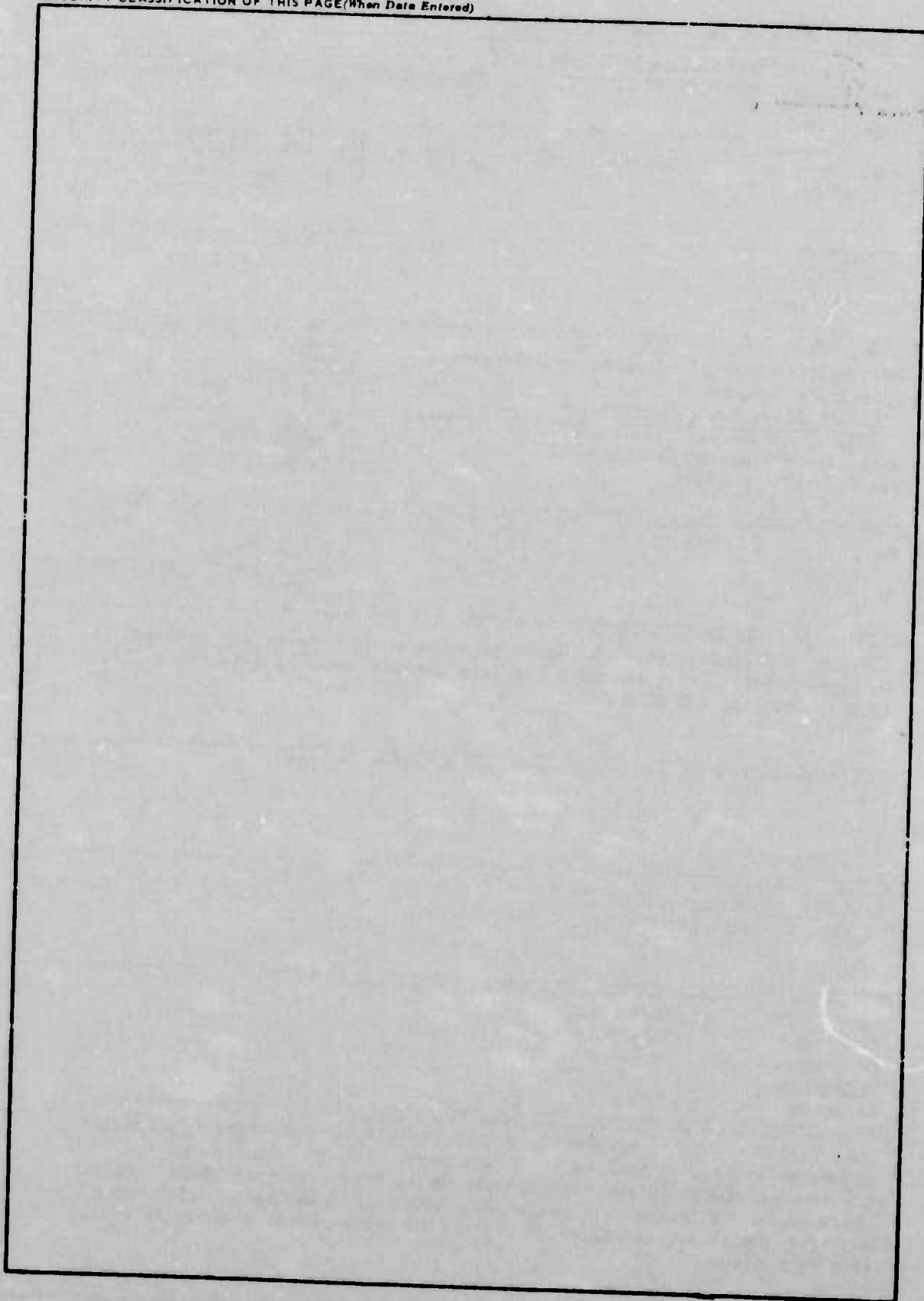
SECURITY CLASSIFICATION OF THIS PAGE (When Data Entered)

19 REPORT DOCUMENTATION PAGE		READ INSTRUCTIONS BEFORE COMPLETING FORM
18 1. REPORT NUMBER RADC-TR-75-247	2. GOVT ACCESSION NO.	3. RECIPIENT'S CATALOG NUMBER 2
4. TITLE (and Subtitle) DEVELOPMENT OF ENCLOSED WIRE INTRUSION DETECTION TRANSDUCER,		4. TYPE OF REPORT & PERIOD COVERED Final Technical Report. 1 May 74 - 28 Feb 75
7. AUTHOR(s) Fred S. Geil Heinz Gilcher	15	5. PERFORMING ORG. REPORT NUMBER N/A 6. CONTRACT OR GRANT NUMBER(s) F30602-74-C-0114 new
9. PERFORMING ORGANIZATION NAME AND ADDRESS Westinghouse Electric Corporation/Electronic Protection Systems 1111 Schilling Road, Hunt Valley MD 21030	16 AP	10. PROGRAM ELEMENT, PROJECT, TASK AREA & WORK UNIT NUMBERS 62702F 6515000-17 651513
11. CONTROLLING OFFICE NAME AND ADDRESS Rome Air Development Center (OCDS) Griffiss AFB NY 13441	11	12. REPORT DATE Sep 1975 13. NUMBER OF PAGES 70
14. MONITORING AGENCY NAME & ADDRESS (if different from Controlling Office) Same	12 74p.	15. SECURITY CLASS. (of this report) UNCLASSIFIED 15a. DECLASSIFICATION/DOWNGRADING SCHEDULE N/A
16. DISTRIBUTION STATEMENT (of this Report) Distribution limited to U. S. Gov't agencies only; <u>proprietary</u> information; <u>September 1975</u> . Other requests for this document must be referred to RADC (OCDS), Griffiss AFB NY 13441.		
17. DISTRIBUTION STATEMENT (of the abstract entered in Block 20, if different from Report) Same		
18. SUPPLEMENTARY NOTES RADC Project Engineer: William F. Gavin Jr. (OCDS)		
19. KEY WORDS (Continue on reverse side if necessary and identify by block number) Line Sensor Surveillance Electret Transducer Capacitance Intrusion Detection		
20. ABSTRACT (Continue on reverse side if necessary and identify by block number) This report covers experimental work on the wire-in-tube buried intrusion detection system, as well as the development of four prototype units which are to be included in the testing program at Rome Air Development Center. These units are fairly well optimized, except for electret consistency and whatever signal processing circuitry may be recommended as a result of the testing program.		

409 513 ✓

UNCLASSIFIED

SECURITY CLASSIFICATION OF THIS PAGE(When Data Entered)



UNCLASSIFIED

SECURITY CLASSIFICATION OF THIS PAGE(When Data Entered)

TABLE OF CONTENTS

	Page
1. INTRODUCTION AND OPERATING PRINCIPLE	1
2. METHODS OF DETECTING THE CAPACITANCE CHANGE INCLUDING THE USE OF BIAS VOLTAGES AND THE INTERNAL POLARIZATION OF CERTAIN INSULATION MATERIALS.	3
3. COMPARISON BETWEEN STRUMMING AND DISPLACEMENT MODES OF DETECTION	8
4. THE USE OF SINGLE VERSUS TWISTED PAIRS OF WIRES	10
5. MEASUREMENTS OF INTRUSION SIGNATURES OF HUMANS.	13
6. EFFECTS OF NOISE SOURCES SUCH AS WIND, TREES, 60 Hz POWER, AND VEHICLES ON THE SENSOR.	16
7. PREDICTION OF LONG-TERM EFFECTS ON THE OPERATION OF THE CABLE	19
8. METHODS OF CONTROLLING THE SENSITIVE WIDTH OF A WIT SENSOR CABLE	20
9. SUGGESTED ADDITIONAL DEVELOPMENT EFFORTS.	21
FIGURES	
APPENDIX A - INSTRUCTION MANUAL FOR R.A.D.C. INSTALLED EQUIPMENT	

EVALUATION

The objective of this effort was to investigate a technique for the development of a line transducer that showed promise for both reliable operation in frozen ground and ease of installation. The transducer consists of an insulated wire loosely laid within a hollow metallic tube. Vibration of the loosely laid wire, caused by an intruders footsteps, results in a change in capacitance between the wire and the outer metallic tube that is easily detectable.

This study investigated several configurations for possible use in Base and Installation Security Systems applications. The configuration chosen for delivery is the easiest to manufacture and requires the simplest electronics for operation. The four transducers delivered are undergoing an evaluation program to obtain a better understanding of the principle of operation, obtain a signature data base on a variety of targets and non-targets and to determine the necessary work to develop this transducer into an operational sensor. Assuming a successful evaluation program, this work would be transitioned to an advanced development program. This work was accomplished under RADC Technical Planning Objective-7.

William F. Gavin, Jr.
WILLIAM F. GAVIN, JR.
Project Engineer

1. INTRODUCTION AND OPERATING PRINCIPLE

The wire-in-tube or WIT sensor consists simply of a metallic tube with an insulated wire loosely laid within it. This arrangement forms a distributed capacitor, whose nominal capacity may be changed by a deformation or mechanical disturbance of the tube, as long as there is a net change in the wire-to-tube geometrical relationship.

Since the insulated wire is loosely laid, it does not mechanically contact the inside of the tube at all points, but only periodically. Next to each touching point is a region of high capacity and mechanical freedom, which provides sufficient sensitivity to enable the detection of a capacity change due to a person walking across a region containing a WIT sensor. The buried depth is approximately eight inches; the sensor length may be one hundred meters or more.

There are several mechanisms for producing a change in the wire-to-tube relationship. First is called the displacement mode. As an intruder crosses the ground above the sensor, the depression of the earth causes a slight bending of the tube. The resultant shifting of the wire between the touching points is enough to produce a readily detectable capacity change, which occupies the frequency band below 1 Hz. The second mechanism has been named by us as the "strumming" mode. Impact of the intruder's footsteps causes the wire to vibrate or "strum" between the touching points. These natural frequencies are in the 20 Hz to 100 Hz band. Above these frequencies lies the accelerometer mode, whereby the inertia of the free parts of the wire causes these parts to tend to remain stationary while the tube vibrates relative to them.

Both the displacement and strumming modes have interest for intrusion detection applications, if the capacity changes can be easily detected. Although there are methods of directly detecting

capacity changes, we have decided instead to transform the capacity changes to voltage changes. This can be done by biasing the wire with a high voltage impressed through a large resistor (the technique used with condenser microphones), or by choosing an insulating material which contains trapped charges, such as Teflon insulation. Microphones that use the technique of trapped charges are known as "electret" condenser microphones. The internal charge can be trapped by heating the dielectric above the curie point and cooling it while in the presence of an electric field. A certain amount of charge is trapped, however, through the normal manufacturing process for Teflon covered wire, and we have found this electret charge equivalent to several hundred volts of bias, providing ample sensitivity for intrusion detection with only modest amplifier requirements. This electret bias appears to be adequately stable with time, after an initial decay in sensitivity encountered after manufacture.

The scope of work on this contract includes some experimentation to optimize the WIT configuration, and the construction and delivery of four 100 meter systems suitable for testing by the Air Force.

Some of the following material is proprietary in nature, representing work done that is outside of the scope of this contract. These paragraphs and figures have limited rights and are indicated as such by the symbol "LR" in the margin adjacent to the paragraph or figure in question.

2. METHODS OF DETECTING THE CAPACITANCE CHANGE INCLUDING
THE USE OF BIAS VOLTAGES AND THE INTERNAL
POLARIZATION OF CERTAIN INSULATION MATERIALS

The first series of tests was done in the laboratory. These tests were conducted to further our knowledge of the electret wire and the particular configuration which we have been using.

Figures 1 thru 5 demonstrate the signal response of a 6 ft long, 1/4" O.D. WIT (wire-in-tube) line sensor using various wire sizes. Note that the #26 wire had the best overall response, especially to low frequency excitation. The data on these figures has been normalized to 200 V for comparison purposes. The instrumentation used to generate these relationships is shown in Fig. 6. Here, a vibrator is driven by a power frequency generator to a desired frequency and amplitude as monitored by the oscilloscope connected to the pickup coil. The WIT output is connected to a high input impedance amplifier, the output of which is connected to an oscilloscope for monitoring. As the frequency is varied throughout the range of interest, the amplitude is adjusted to compensate for mechanical resonances and other effects.

In order to aid the mechanical optimization of the WIT line LR sensor, a mathematical model was developed which relates the distance between wire touch points, limpness, and mass to sensitivity as follows:

$$\frac{\Delta C}{C_0} = K(\rho/E)(L/R)^4$$

where ρ = mass per unit length of wire
 E = Young's modulus of the wire material
 L = distance between touching points
 R = radius of the wire
 K = proportionality constant.

This equation shows that sensitivity is maximized by using small yet high density wire, which is limp but with widely spaced touching points.

While we cannot optimize each variable without affecting others, it is
LR clear that aluminum wire would not be the choice because of low mass, and
steel wire would tend to be excessively stiff. In addition to the math model,
a glass WIT line sensor model was assembled to improve our knowledge of the
actual wire-tube mechanical configuration. Wires were pulled through
this tube and their resulting lay characteristics with respect to touch
points were observed. In order to provide for a more consistent mech-
anical wire-tube configuration, several attempts were made to put
periodically spaced kinks in some WIT wire samples. These wires were
pulled into the glass tube model for visual inspection and later were
performance tested in a metal tube. Since this test was only marginally
successful, no further effort was expended at this time.

In order to provide for a more uniform sensitivity along the
length of a WIT line sensor, a test device was developed for evaluating
the charge potential on wire electrets. The test setup shown in Fig. 7
consists of a power frequency generator driving a mechanical vibrator which
varies the capacitance between a small, thin metal plate and the wire
under test. The plate which is 1/2" square is mounted on insulating
material as shown. The electret wire is drawn through a set of spring-
loaded rollers for mechanical positioning purposes. A permanent magnet
is connected at the end of the vibrator drive rod. This magnet induces
a coil signal voltage proportional to the vibration amplitude. The coil
output signal is monitored with #1 oscilloscope. A variable high voltage
power supply is connected to the wire as shown. The power supply is
adjusted to provide a null signal as monitored on #2 oscilloscope. The
resulting power supply bucking voltage equals the electret charge
potential on the short section under test independent of small mechanical
misalignment. The wire can be advanced in short increments and a charge
potential profile such as shown in Fig. 8 can be developed. Note that
this length of wire had an electret potential variation exceeding 5 to 1.
Note also that the repeated tests, run in the same direction but at
different wire angles, have similar trends. This degree of electret
potential variation can cause considerable line sensor sensitivity varia-
tion depending on the location of the wire touch points on the tube wall.

An electret study was performed independent of this contract LR in an attempt to produce our own improved electret wire. As part of this effort a wire sample was heat treated to drive off the electret charge. The wire was tested to determine the amount of residual electret charge remaining as shown in Fig. 9. The maximum electret potential remaining on the wire was about 90 volts, which is considerably lower than the +600 V maximum before heat treatment. This wire was also tested with the power supply set to 0 V and -500 V, and the resulting output signals from the vibrating plate were also plotted as shown. As might be expected, the zero bias plot appears to have a shape similar to the residual electret potential curve. The -500 V bias plot has a relatively consistent behavior, the variation being caused primarily by dimensional differences in the wire. Using first a prolonged heat treat period followed by a prolonged period of high voltage bias across the wire insulation while slowly cooling the wire to room temperature, we were able to form a fairly good wire electret which held its charge potential over a prolonged period of time. The potential variation along its length, as shown in Fig. 10, was better than that of the electret as received from the manufacturer. Our fabricated electret's potential variation was primarily due to a nonuniform electrode around the wire insulation during the electret forming process.

In order to avoid some of the possible technical problems associated with electret technology, it was thought that a nonelectret voltage biased wire could serve equally well in the WIT sensor application. A circuit for biasing a WIT wire which is compatible with the amplifier input, is shown in Fig. 11. The .47 μ F filter capacitor and the .1 μ F coupling capacitor are very critical components in this circuit configuration. Unfortunately, standard good quality capacitors of the proper voltage rating generate spike transient noise believed to be associated with momentary realignment of dielectric domains. This is a high impednace phenomenon since such behavior does not show up in circuits of moderate impedance. In this case the D.C. input impedance is 100 M Ω . The capacitors finally chosen were Sprague Type 118P Difilm

metalized capacitors which are designed to have very good performance with regard to self generated noise. These capacitors were successfully used for our amplifier application.

Another source of input signal noise is associated with the transmission of a high voltage bias to the preamplifier via a buried cable. If any pin-holes exist or if any cable damage occurs, the resulting leakage can cause the high voltage bias line to introduce noise into the preamplifier. This condition is especially true when the bias supply has a high output impedance.

A technique which would get around the long transmission line problem would be to build a small low voltage to high voltage converter in the preamplifier package. This converter would operate at a high frequency and would require good shielding and adequate filtering.

Another approach, should one decide to go to such a degree of sophistication, would be to use a neutral wire WIT as the capacitor in a tank circuit of a frequency modulated system. This would also have the advantage of being a low input impedance system.

Some buried sensor tests were performed to determine the differences between the electret technique and the voltage bias technique. These tests were run on 50 ft line sensors. The results showed that variation of sensitivity along the sensor length due to linear electret charge variation showed little significant difference compared to the voltage bias tests. The differences in sensor burial and in ground conditions seemed to swamp out this variable. Figure 12 illustrates a test setup in which we attempted to determine the exact transition point of a split buried line sensor by making successive intrusions in the vicinity of the transition point. We determined that intrusion crossings somewhat distant from the transition point generate signals in both halves of the split sensor. This situation indicates that a relatively long length of the electret wire, compared to the length of wire involved in natural electret potential charge variations, is disturbed during intrusions. It thus appears that an intrusion tends to integrate the effects of abrupt electret potential variations. One of our two parallel installed

300 ft WIT line sensors has low sensitivity over a long length. This low sensitivity is caused by a relatively long, low charge potential electret wire and indicates the need for more uniform electret wire.

No significant variation of signature frequency characteristics along an installed WIT line sensor due to electret charge variation could be detected from our tests.

3. COMPARISON BETWEEN STRUMMING AND DISPLACEMENT MODES OF DETECTION

A series of lateral sensitivity profiles were developed to determine the performance range of the WIT sensor in a variety of ground conditions. This data was generated with a combination of step responses (long board bridging sensor with person stepping down at one ft. intervals), impact responses (intruder jumping at fixed intervals), and ordinary intrusion crossings. A typical set of sensitivity profiles is shown in Figs. 13, 14, 15, and 16. Note that the data is normalized so that the maximum crossing sensitivity (directly over the sensor) is set at 0 dB. These profiles can be compared only in terms of their general shape. Due to the variation of ground conditions along a sensor length and the variation of intrusion types (from run to slow creep), profile sensitivity comparisons, even under the same weather conditions, show variations. These figures are divided between high frequency and low frequency bands. The low frequency or displacement mode occupies the frequency band below 1 Hz, while the high frequency band, or strumming mode, occupies the 20 Hz to 100 Hz band. In comparing the two low frequency lateral sensitivity profiles, it is apparent that the wet profile response, as distance from the sensor is increased, drops off at a greater rate than the frozen profile response. At the point directly over the sensor, the low frequency frozen profile response can be about 20 dB less sensitive than the low frequency wet profile. At some lateral distance from the line sensor (e.g., zone boundary), which is a more practical location for sensitivity comparison, these low frequency sensitivities would be more nearly equal. The two high frequency lateral sensitivity profiles are more similar except that the high frequency wet profile has a high sensitivity peak directly over the sensor. The high frequency frozen profile response, although more flat, is somewhat more sensitive at greater distances from the sensor.

The nuisance sources that influence the low frequency mode are large trucks passing within several feet of the sensor and tree root noise caused by high wind when the sensor is located near large trees. When there are no trees near the line sensor and vehicular traffic is at reasonable distances, the low frequency mode is relatively immune to these nuisance sources. The nuisance sources that influence the high frequency mode of operation are nearby industrial machinery (25 to 50 ft depending on vibration level), heavy trucks, low flying aircraft, and loud thunder. The extent of influence of these sources depends upon the alarm threshold levels needed.

4. THE USE OF SINGLE VERSUS TWISTED PAIRS OF WIRES

Early in the WIT line sensor development a scheme using a twisted pair of electret wires inside a metal tube housing was devised to cancel out unwanted distant disturbances beyond a desired zone width. A simplified version is shown in Fig. 17. It is made up of two wires in a tightly twisted configuration which have alternating electret (active) and passive sections. The solid lines represent the active sections; the dotted lines signify the passive sections. The wires are connected to the + and - inputs of a differential amplifier. When a distant (noise or nuisance) disturbance occurs, a relatively long length of the WIT sensor is excited, and both wires produce nearly equal output signals (since they are tightly twisted). These signals, differentially amplified will tend to cancel. However, when a disturbance occurs relatively close to the sensor, the closest section will produce the major response, which will result in unequal inputs to the differential amplifier. The output from the differential amplifier is processed by the alarm detector.

In order to determine the practicality of using the twisted pair differential technique, we first performed a series of bench tests to determine if further testing of this configuration in a buried sensor form would be warranted.

Some twisted pair WIT sensor bench tests were performed with the apparatus shown in Fig. 6. The tube section was about 6 ft long and open at both ends to permit ease in changing wire types. Two 6 ft twisted pair wires were made up. One twisted pair was made up of #26 teflon insulated electret wire as provided by the manufacturer, while the second twisted pair was made up of annealed #26 teflon insulated wire (a non-electret). The twisted pair electret frequency response is shown in

Fig. 18. Note that the signal from each wire of the pair is plotted. The output from each wire is fed to a differential amplifier (unity gain) and the output difference signal is plotted as shown. The same test is run on the nonelectret wire except that a -500 V bias is applied on each of the wires. The frequency response for the nonelectret pair is shown in Fig. 19, along with their differential output. Note that the signal response for both twisted pair samples drops off severely below 25 Hz. This is due to the relatively large diameter of the twisted pair compared to the inner diameter of the tube. One would use a smaller wire size in making up a practical WIT twisted pair sensor. The shape of both twisted pair response curves is similar. However, the difference amplitude outputs are not similar. The nonelectret twisted pair does a better job of producing similar signals in both phase and amplitude. This can be further seen by a common mode rejection ratio versus frequency plot shown in Fig. 20. Common mode rejection ratio is defined here as the average of the twisted pair wire output signals in volts p.p. (not considering phase) divided by the differential amplifier output in volts p.p.

$$CMRR = \frac{|V_1| + |V_2|}{2(V_1 - V_2)}$$

The nonelectret twisted pair C.M.R.R. is considerably higher than that of the electret twisted pair indicating that if a twisted pair arrangement is used, it should be made up of very uniform electret wires or voltage biased nonelectret wires.

With this reasonable laboratory bench test success, we decided to transfer further testing to the field using some long-established 50 ft line sensors. The ends of these sensors were accessible for ease of replacing wires. In our first test, we made up a 50 ft long nonelectret twisted pair using #26 teflon wire. Each wire was independently biased to -500 V. A series of tests was performed which demonstrates the performance of this buried twisted pair WIT sensor as shown in Fig. 21. The run and walk signals from both channels look almost

identical. The impact signals at 2, 4, 6, and 8 ft from the sensor also appear alike, but better definition is needed to compare the high frequency signature on a cycle by cycle basis. Figs. 22 and 23 illustrate a higher speed record of channel 1 impact signature and the differential amplifier output resulting from taking a channel 1, channel 2 difference. The impacts (person jumping) were made at 2, 4, 6, and 8 ft distances from the sensor as shown. The rejection capability of this buried sensor or the C.M.R.R. ranges between 6.8 and 8.7.

We consider these results very encouraging and decided to conduct the final test of this series with a sensor configuration as similar as possible to that shown in Fig. 17. Since the voltage bias technique cannot be used in this configuration, and since we have not been able to produce a suitably uniform electret at this time, we set up an equivalent experiment as shown in Fig. 12. In this configuration the buried 50 ft line sensor is made up of two 25 ft nonelectret voltage biased teflon wires which are mechanically connected and electrically separated. Each wire is connected to an amplifier as shown. Since most unwanted distant signals are high frequency in nature, impact jumps were made at four foot intervals from the line sensor in a line perpendicular to and crossing the center of the sensor as shown. The resulting signals from both amplifiers are shown in Figs. 24, 25, and 26. In comparing the output signals for a particular impact, it becomes obvious that on a cycle per cycle basis, distant signals cannot successfully be balanced out. If these signals were envelope detected, it appears that a significant improvement could be made. Considering the amount of further development needed to make a successful twisted pair differential WIT line sensor, no additional effort was expended in this direction.

5. MEASUREMENTS OF INTRUSION SIGNATURES OF HUMANS

A variety of human intrusions were made which included walks, runs, creeps, and slow creeps. These tests were performed in a quiet zone at Westinghouse R&D duck pond area. This test site is enclosed by fencing and is distant from any industrial noise sources. The two parallel buried WIT line sensors which are about 300 ft long, are connected to 40 dB low noise preamplifiers. The preamplifier outputs are connected to additional amplification located several hundred feet away in a pump house. A wind speed indicator and our recording equipment are also set up at this location. Several dedicated telephone lines are connected from the pump house to our laboratory in order to monitor the system for long time periods, particularly during unusual weather conditions.

The human intrusions were made at six equally spaced stations or posts along a fence paralleling the line sensors. These posts are at 40-50 ft intervals and are numbered 1 to 6, starting at the amplifier end of the line sensor.

All of the intrusion data was recorded with a TEAC portable multichannel F.M. cassette magnetic tape recorder. The data was recorded on at least two channels. The second channel was recorded at an additional 10 to 20 dB of gain in order to provide for a large dynamic range in order to maximize the recorded signal-to-noise ratio.

Spectral analysis instrumentation was set up to perform a Fast Fourier Transform of the recorded intrusion signatures. This instrument system consisted of a Tektronix 7704A/P7001 Digital Processing Oscilloscope (D.P.O.) and a P D P-11/05 Digital Computer. This system was programmed to accept a selected sampling time period of magnetic tape intrusion output data and put it into digital storage. This sample time is adjustable over a wide range. After a sample of intrusion

data was put into storage, the FFT data processing was performed, and a spectral response was generated on the oscilloscope display. A large number of intrusion spectra were photographed and a representative sample of this data is shown in Figs. 27 thru 31, inclusive. Note that each spectral response photograph has additional printed information regarding the run along the top and bottom edges. In Fig. 27 the upper left display, for example, has P3 RUN 3 MIN. appearing along the lower edge. This refers to the post 3 location, the third run out of a total of six, which also had the minimum signal amplitude of the six crossings. The +3 Div. refers to three large divisions above the scope zero level as being the reference which is indicated as the 0 dB level. Appearing near the upper display edge, the 10 DB RE 1 V. 128 HZ R.H. EDGE refers to the large graticule divisions being 10 dB, the reference voltage being 1 V at 0 dB, and the frequency at the right hand graticule edge being 128 Hz. The negative going vertical marks from the uppermost scan line mark octaves down from the right-most graticule mark (128 Hz). Note that the various figures do not have the same frequency set at the right-most graticule mark. This variation in setup was made to best accommodate the type of intrusion being performed. Each intrusion of the line sensor included several footsteps all of which are summed to obtain a total frequency response for a crossing. On examining the four types of intrusion spectra shown in Figs. 27 thru 30, the trend for damp ground conditions is that as the intrusion types change from runs to walks, creeps, and then slow creeps, the spectra change from having greater high frequency content to almost total low frequency content. There seem to be no apparent sharp peaks in this data, which would indicate a particular strumming mode, although there is high frequency signal present. Averaging of the six intrusions has a tendency to smooth out the spectral data.

Some additional spectral signature data was taken shortly after a wet snow fall. The spectral response of this data is shown in Fig. 31. In comparing these walk signatures with those shown in Fig. 28, considering a 10 dB gain difference, there seems to be little significant change due to these ground differences.

After the WIT system was installed at R.A.D.C., some intrusion data was recorded on magnetic tape. Some of this recorded data was spectrum analyzed and photographed. Since there was about 12 inches of snow on the ground and the temperature was at 32°F when the signature data was taken, the signal spectrums appear different than those taken earlier. The high frequency content in the 20 to 100 Hz range is 20 dB higher, while the low frequency content was about 20 dB lower.

6. EFFECTS OF NOISE SOURCES SUCH AS WIND, TREES,
60 Hz POWER, AND VEHICLES ON THE SENSOR

There is a discussion on the effects of trees, wind, and vehicles in section three. In addition it has been observed that in the presence of trees, the high frequency mode is not influenced by tree root noise. In open areas, wind noise is negligible in both the low and high frequency mode. Although industrial and vehicular noise can be detected at greater distances in the high frequency mode, these types of signals can be envelope detected and discriminated against. (Both high frequency industrial and vehicular noise appears closer to a continuous wave signal compared to an intruder's high frequency signature which is more burst-like.)

Figure 32 is a comparison of a 300 ft WIT line sensor response to various rain conditions. (The system gain was turned up to 80 dB to achieve a proper recording level.) At the upper left is an average spectral response with no rain. To the right is an average response with light rain, and at the bottom is an average response with heavy rain. The light rain response is almost identical to the no rain response except that at 50 Hz the light rain signal is about 10 dB greater. The heavy rain spectral response is slightly higher and fairly continuous over the display spectrum.

Figure 33 is a comparison of a creep intrusion and light rain noise spectrum. The light rain noise spectrum is offset to compensate for differences in recording gain. Note that the noise is 10 dB or more below the lowest signal level. A wide band spectral response is shown in Fig. 34 which is an average of six samples of very heavy rain. Since a heavy rain is random in nature, the resulting spectrum amounts to a transfer function of a 300 ft buried WIT line sensor. The higher frequency portion of the display indicates the system response in an audio listening mode.

The 300 ft WIT line sensor and associated system were monitored several times during severe electrical storms. No significant lightning signal was picked up by the system. (An early system was destroyed by a near-direct hit. The protection circuitry has since been improved.)

Since the WIT line sensor is electrical in nature, it was decided to run some tests to determine the effects of 60 Hz ground currents usually associated with areas near buried power lines. The results showed that if isolated 60 Hz power line current of 0.5 amps is permitted to flow through the outer tube conductor of a 50 ft line sensor, significant signal pickup is experienced. The mechanism by which the noise pickup occurs is capacitive in nature.

As mentioned earlier, our WIT sensor at the pond test site can be monitored in our lab area. With this arrangement, long-term monitoring runs were conducted to provide background noise data during weather changes.

While these tests were being conducted, large single noise spikes were noted. The occurrence rate would vary from several pulses per hour to one pulse in several hours. After considerable investigation, it was determined that the cause of these noise spikes was a sudden mechanical slippage of the wire with respect to the tube wall which resulted in a step function change in capacitance. After further investigation it was concluded that most of the spike noise was thermally induced by changes in the weather. Changes in the weather cause the ground to create mini-seismic disturbances (ground cracking in hot dry weather or heaving while freezing and thawing).

An attempt was made to record a random spike signal on magnetic tape for later spectral analysis. Figure 35 shows two small spike-like signals and their spectral content. Although the actual noise spikes do not look alike, their spectral content is very similar with noise spike 1 slightly higher in low frequency content. Note that the vertical scales for the spectral responses are displaced from each other, while the 0 dB level is common to both.

It was decided to run some long-term tests whereby the incoming signals were separated into high frequency and low frequency bands with separate alarms for each frequency band. The two frequency bands were separated at 10 Hz, the high frequency including everything above and the low frequency including everything below this frequency. The long-term test results showed that there are significant differences in the spike pulses since some spikes cause a high frequency alarm, some cause a low frequency alarm, and some cause both high and low frequency alarms.

LR Since most noise spikes (positive or negative going) have rapid rise times and similar slow decay times, and since it is known that signal spikes are caused by step function capacitance changes, the decay time constant must be due to the WIT electronic system transfer function. Using this as background, an attempt was made at the Westinghouse Electronic Protection Systems Division to sense these spike noise pulses and buck them out with an equivalent generated spike pulse. This arrangement seemed to work well for the relatively short test period. We do not know if it will perform well for extended tests with a variety of spike pulse types.

LR Another technique for dealing with this type of disturbance involves the use of a circuit which can detect whenever a net change in capacity has occurred and inhibit the alarm circuit. This technique also effectively turns the randomly occurring capacity change into a test signal which includes the sensor as well as the electronics in the test.

LR There are two techniques, as yet untried, for eliminating the capacity changes, by eliminating the wire slippage. The first involves "crinkling" the wire to avoid longitudinal tension build up, while the second technique consists of periodically crimping the tube, in order to anchor the wire at these points. Again excessive longitudinal tension is avoided.

7. PREDICTION OF LONG-TERM EFFECTS ON THE OPERATION OF THE CABLE

The literature seems to indicate that good electrets have a relatively long life (20 to 40 years). Our experience with the WIT sensor configuration is that after an initial decay, the sensitivity remains relatively constant. Our first sensors which were buried in 1972 are still working well.

The mechanical integrity of the cable is such that unless it is damaged by careless backfilling, it should last indefinitely. Rodents, which sometimes damage underground electrical cables, will not disturb the sensor's metallic exterior. The WIT sensor is permanently sealed at both ends after being flushed out with dry nitrogen. The metal tube used for the WIT sensor is leak tested refrigerator tubing and after the sensor fabrication is complete a final leak test is performed. A P.V.C. outer cover is added to the sensor to avoid ground current concentration on the sensor caused by power lines or lightning. The outer cover also provides some degree of mechanical and corrosive protection.

The buried preamplifier and the other associated electronics are provided with transient high voltage protection to insure long life.

8. METHODS OF CONTROLLING THE SENSITIVE WIDTH OF A WIT SENSOR CABLE

The profiles of the WIT line sensor with respect to high frequency and low frequency operation are discussed in Sec. 3. The twisted pair technique for limiting zone width is also fully discussed in Sec. 4.

In addition, the low frequency profile and possibly the high frequency profile can be significantly altered by the depth of burial. Zone limiting can also be accomplished by installing two parallel sensors in differential fashion. Electronic signal processing, whereby high frequency continuous signals from trucks and industrial sites could be ignored and only high frequency footstep pulsed signals accepted, can be implemented. Logic can also be arranged to use the high frequency and low frequency signature signals in logic combinations to achieve zone control.

9. SUGGESTED ADDITIONAL DEVELOPMENT EFFORTS

Sensor Improvements

As indicated in Section 2 above, the sensor may be improved by insuring that a controlled uniform electret charge is achieved in the wire insulation. The benefit from such an improvement would lie in more consistent intrusion signatures from point-to-point along the sensor, which would provide an improvement in detection probability and/or false alarm rate. Unit-to-unit sensor sensitivity variations would be eliminated, permitting the circuit gain to be pre-set to a predetermined level. Such a program should consist of a theoretical/experimental investigation of electret inducement techniques and subsequent measurement of sensitivity decay.

LR

Also noted in Section 6 is a characteristic noise spike which is due to thermally induced movement of the sensor. It is very likely that this noise can be eliminated from the sensor, or it can be discriminated against in the detector electronics. (One such technique can actually make use of the noise to create a self-test capability.) Two techniques for eliminating the noise appear promising. One technique consists of periodic mechanical fixing of the wire in the tube to prevent longitudinal tension buildup and subsequent slippage. The other technique would use an intentionally crinkled wire, also to prevent the tension buildup.

Electronic Improvements

The WIT detector has a high degree of inherent immunity to false alarms at the same time as a high probability of detection rate. Signal processing requirements may be minimal, requiring little more than the "OR" processing furnished with the four prototype sensors.

The testing program underway at Rome Air Development Center will provide an excellent data base from which to predict the performance using optimum filtering of the two frequency bands and either "OR" or "AND" processing, at least within the scope of the noise and nuisance sources monitored. If it appears that more sophisticated techniques are required such as AGC, sequencing of detectors, or signature integration, an appropriate development program may be undertaken, using the taped signatures from the RADC testing program. One additional nuisance source which might be included in such a program is tree root movement due to winds. These signals have been only qualitatively observed to date, but it appears that slightly raising the low frequency cutoff of the low band (perhaps only during windy periods) will be sufficient to deal with the problem. Another approach might be to physically cut or remove the roots in the vicinity of the sensor.

Another useful program would exploit the audio capability of the sensor, in target classification. Being a line sensor, the WIT sensitivity decreases only as the square root of the distance to the target rather than directly as the distance. It is likely that automatic recognition of target types is possible, as well as assessing speeds of moving targets. The feasibility program would employ spectral analysis of various target signatures to indicate classification ability, and construct appropriate prototype hardware.

LR Still another electronic project that might be pursued is the development of inhibit circuitry to cope with the periodic sensor movement noise. An early experiment at the Hunt Valley Division has shown that this noise can be effectively eliminated by a cancellation technique. A better technique may be to use the capacity step change due to the wire shift as a randomly generated test signal, using a capacity-step detector at the preamplifier. Such a self-test method would have the advantage of actually including the sensor in the test function.

10. BIBLIOGRAPHY

1. Patent Disclosure, Gilcher, H., An Accelerometer Cable Sensor for Intrusion Alarm Systems, 1 August 1972.
2. Issued Patent 3,846,780: Gilcher, H., Intrusion Detection Systems, 5 November 1974.
3. Westinghouse Internal Memo, 73-IM7-PERIX-M1, Gilcher, H., Investigation of Intrusion Sensing Electrical Cable, 12 February 1973.
4. Patent Disclosure RES 73-448, Geil, F., and Gilcher, H., High Frequency Uses for the Wire-in-Tube Detector, 30 August 1973.
5. Pending Patent 460227: Geil, F., and Gilcher, H., High Frequency Uses for the Wire-in-Tube Detector, 11 April 1974.
6. Paper, 1974 Proceedings of the Carnahan Conference: Geil, F., and Gilcher, H., Wire-in-Tube Sensor, April 1974
7. Westinghouse Internal Memo, 75-IM7-DFOOT-M1, Skinner, D. D., Electret Improvement for the Wire-in-Tube Buried Sensor, 4 February 1975.

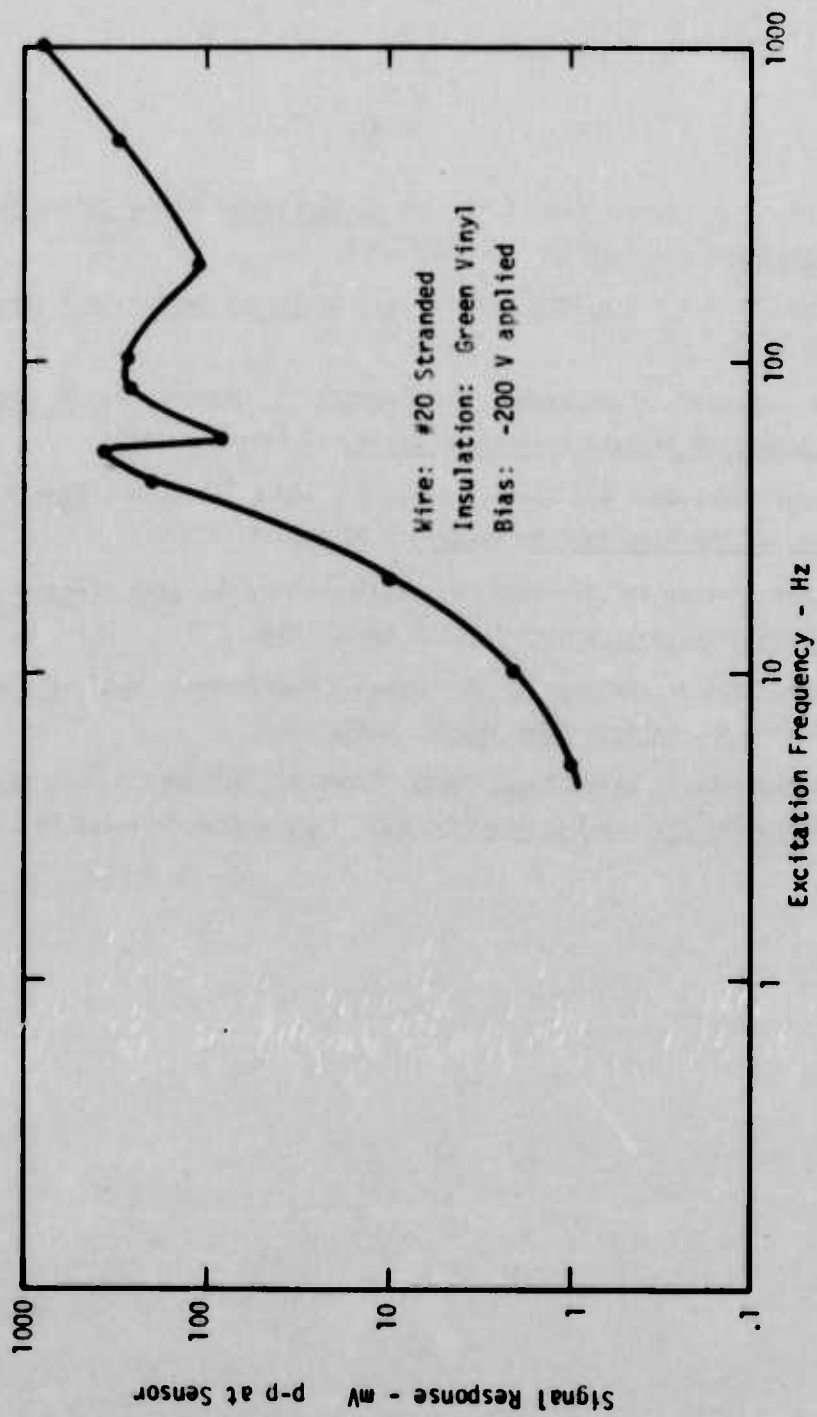


Figure 1 - Frequency response of sample MIT sensor, using apparatus of Fig. 6.

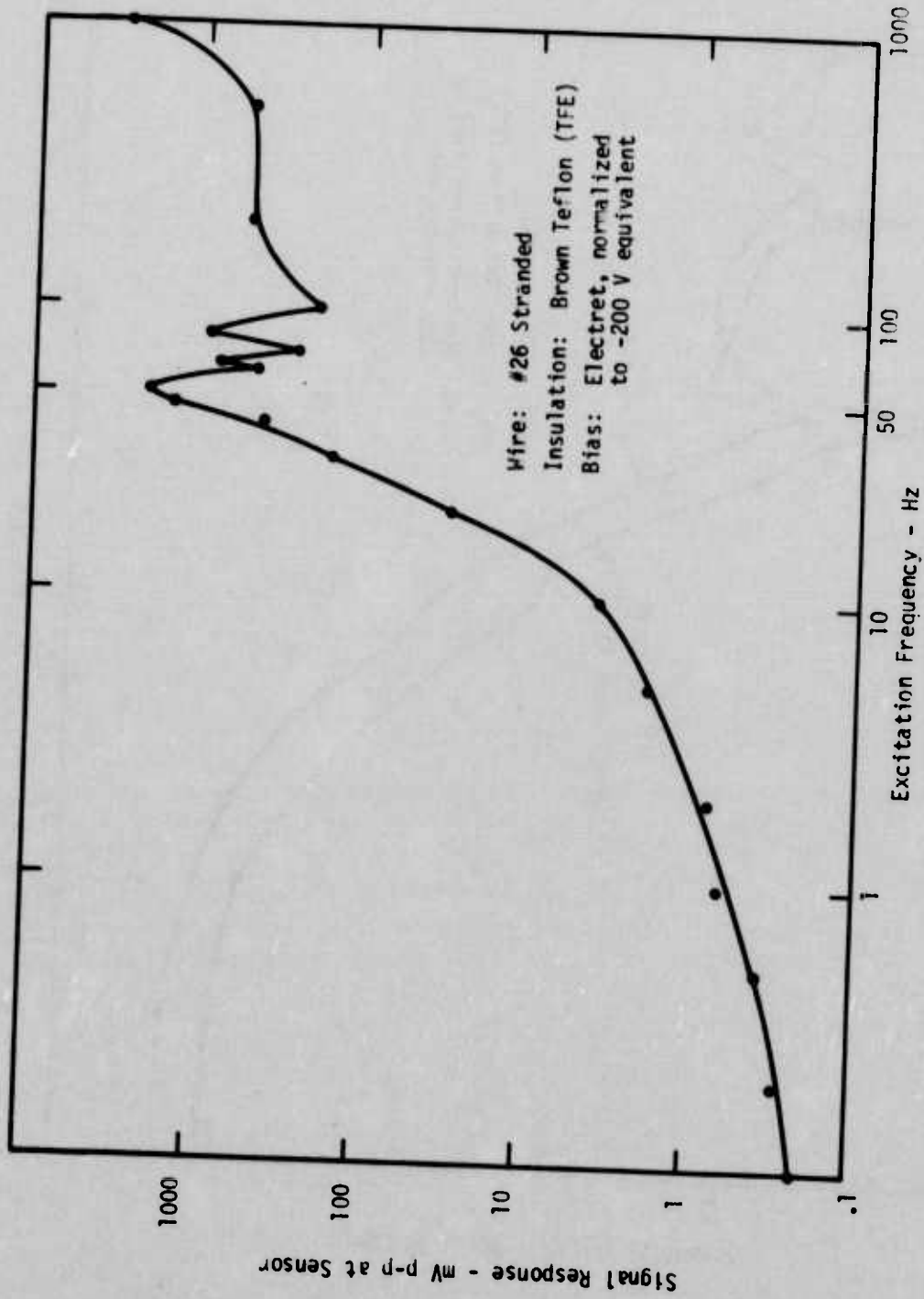


Figure 2 - Similar frequency response for sample using electret wire.

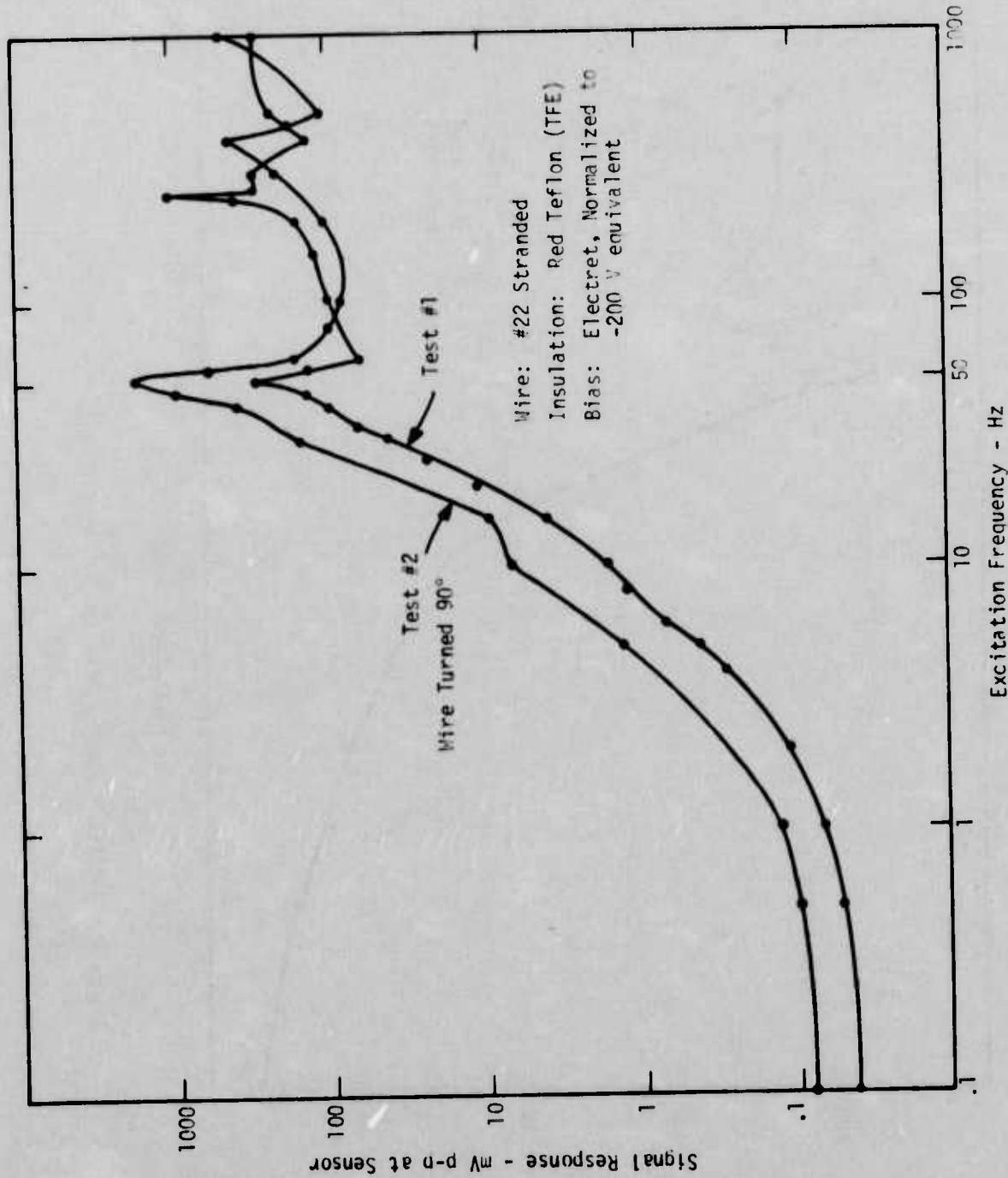


Figure 3 - Another sample frequency response, showing effect of turning wire.

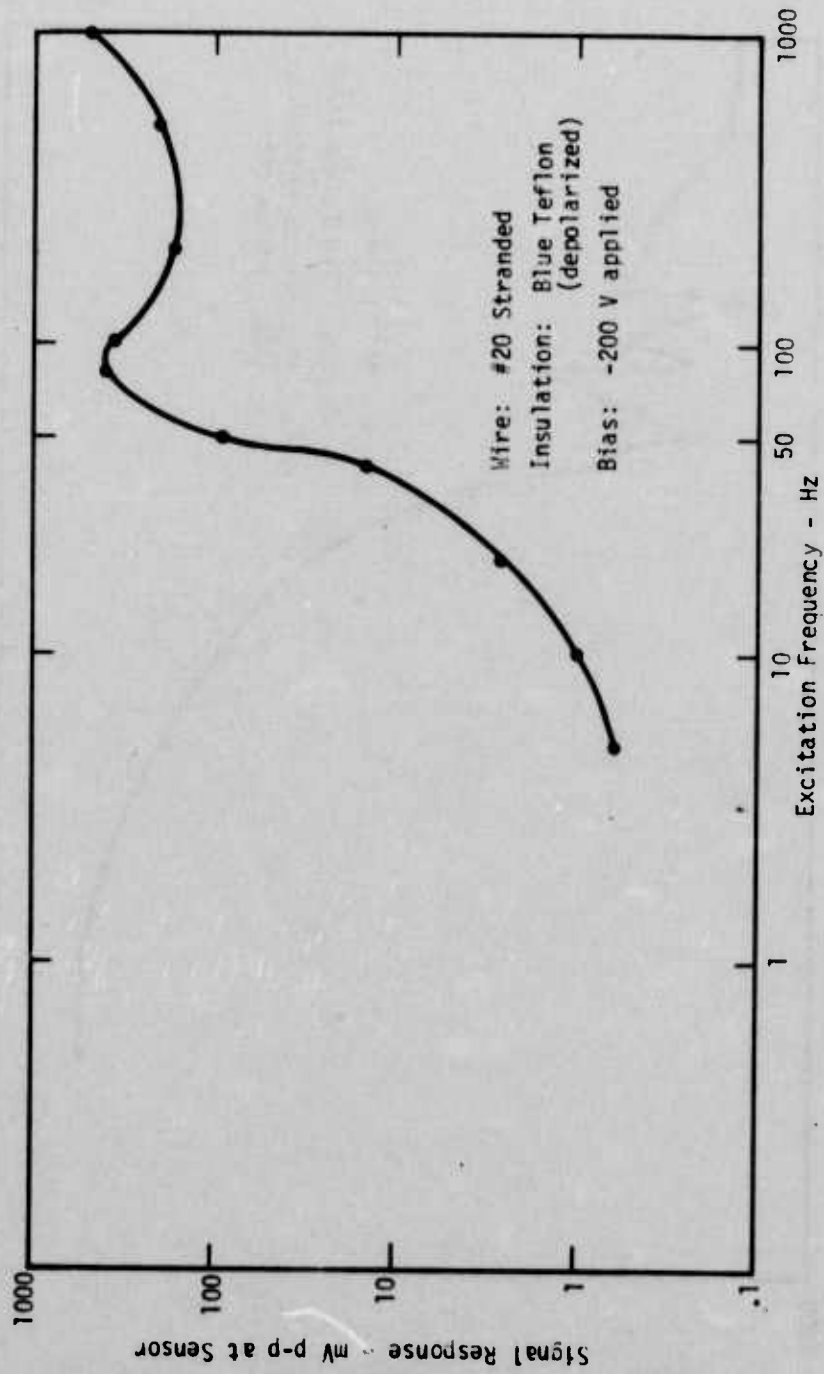


Figure 4 - Frequency response for depolarized, biased, wire sample.

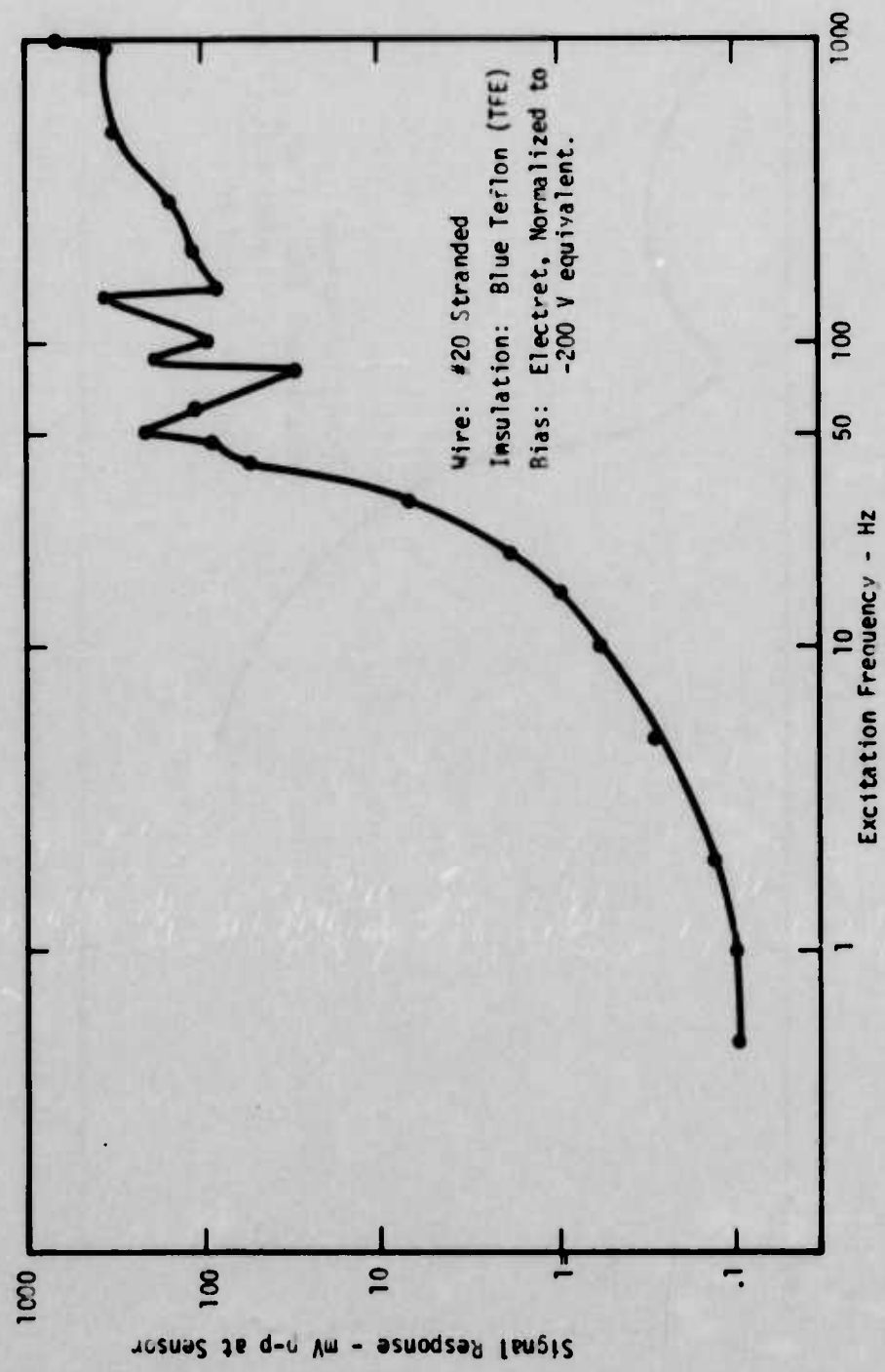


Figure 5 - Similar to Fig. 2, except for larger gauge wire.

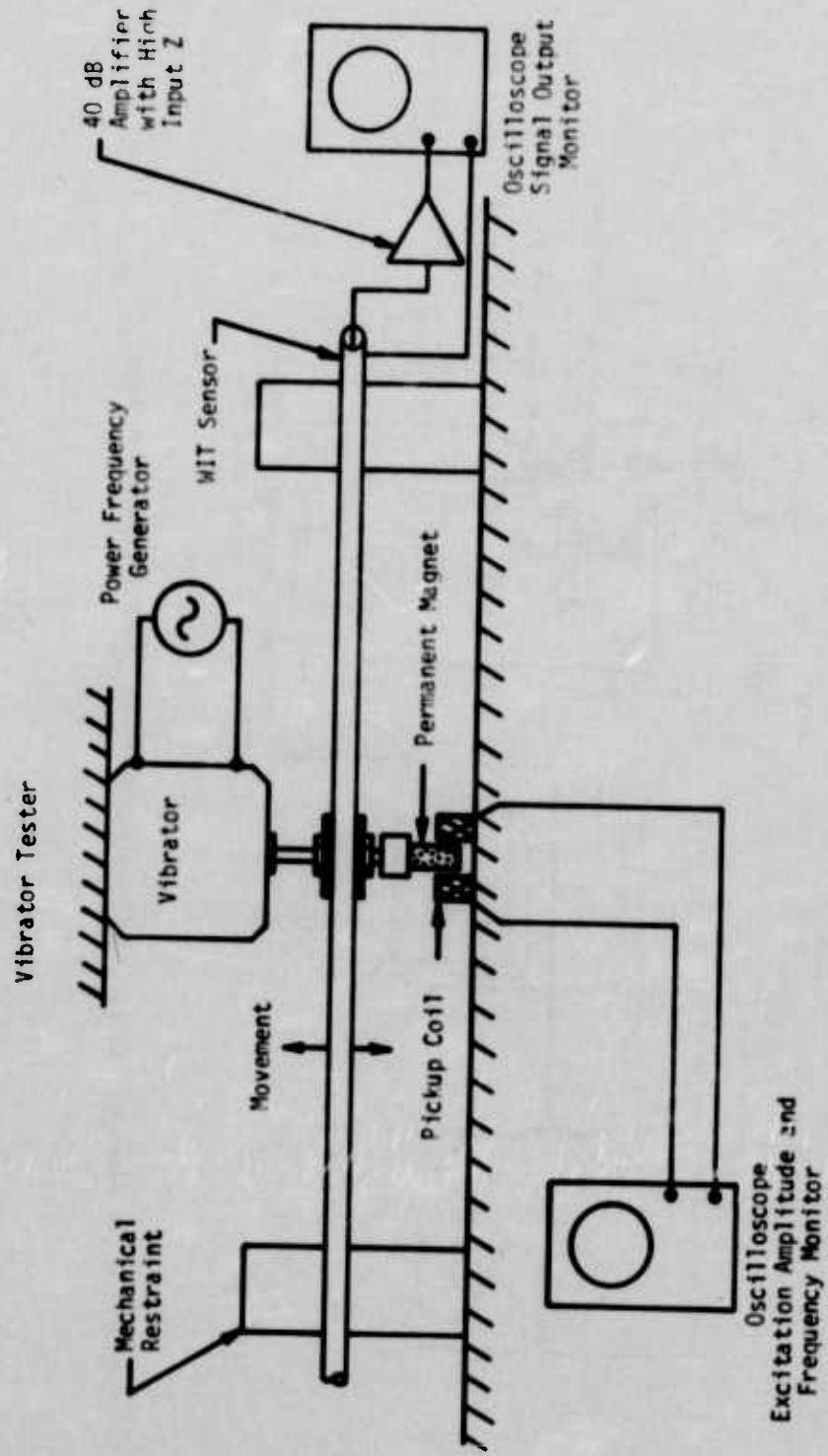


Figure 6 - Test setup for measuring frequency response (Figs. 1 thru 5).

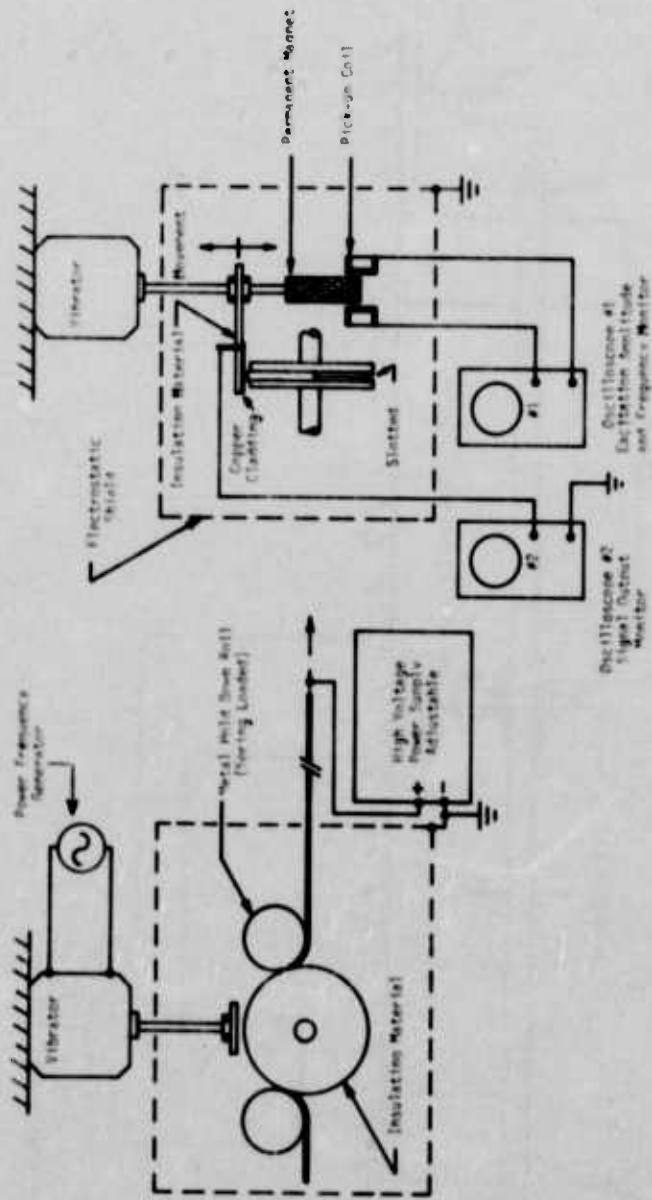


Figure 7 - Two views of instrument for determining electret charge variations.

Curve 678736-A

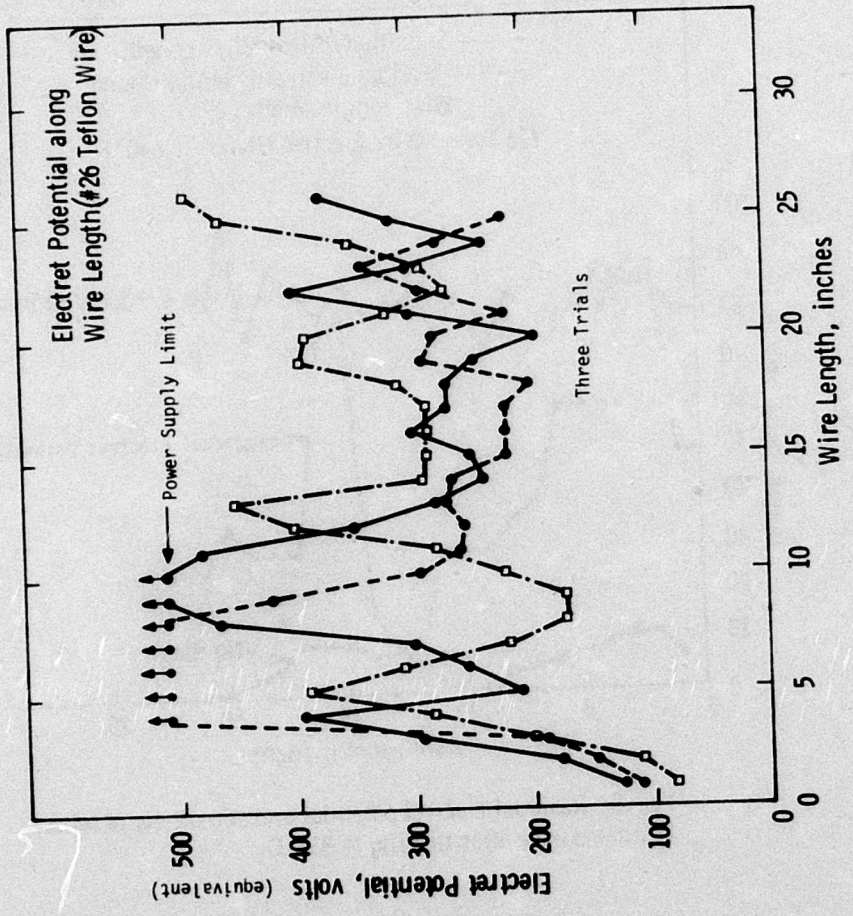


Fig. 8—Electret potential as a function of length for teflon insulated wire as received from the manufacturer

LR

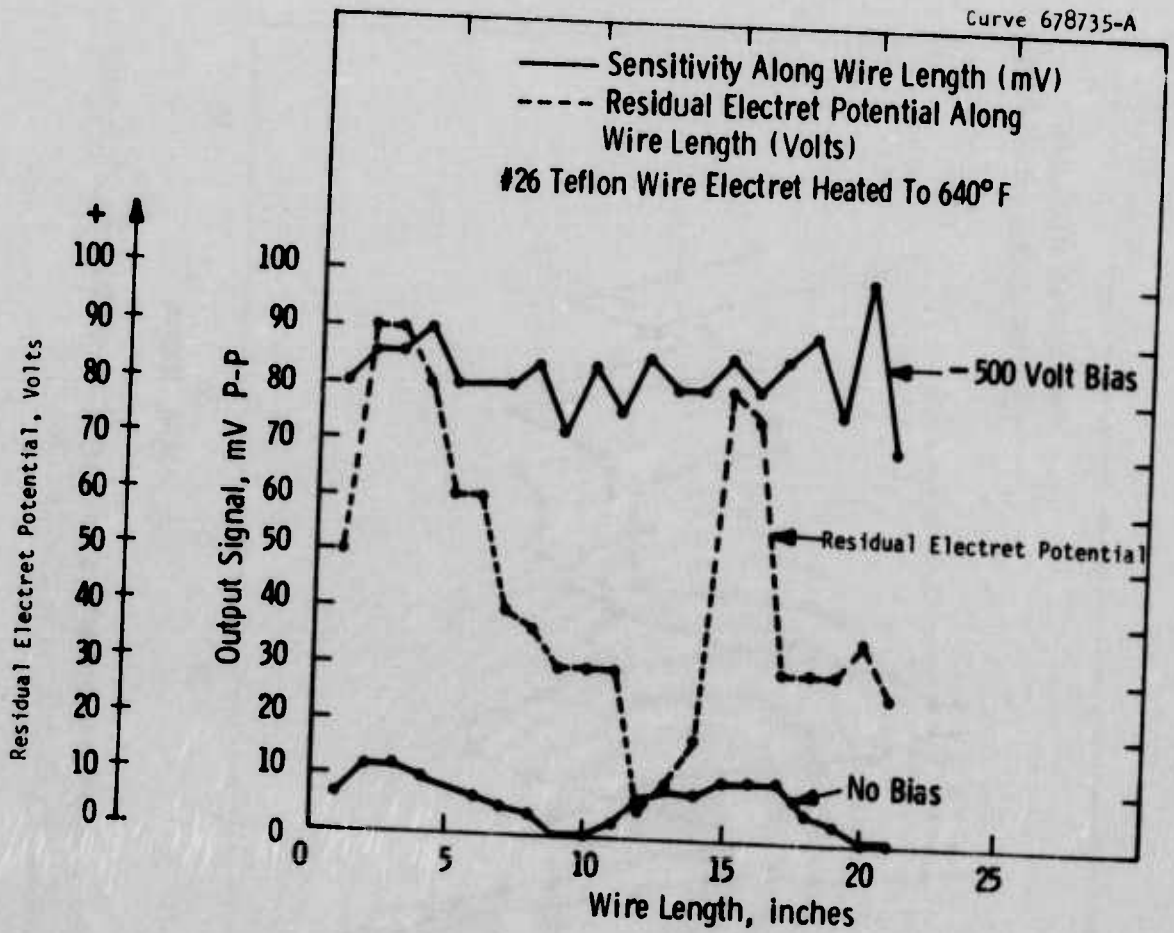


Fig. 9— Residual electret potential and sensitivity of teflon insulated wire after heating to 338° C

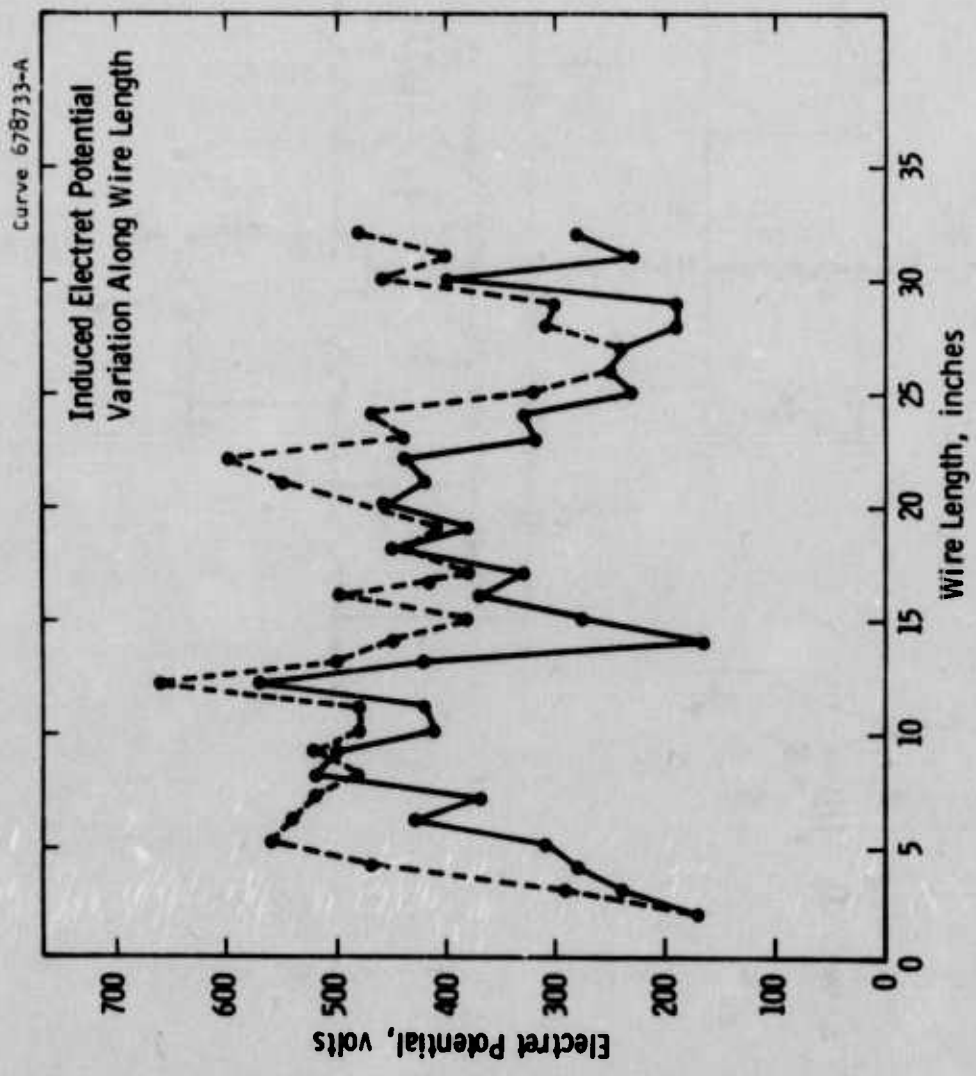


Fig. 10—Electret potential as a function of length for teflon wire polarized with a positive polarity

LR

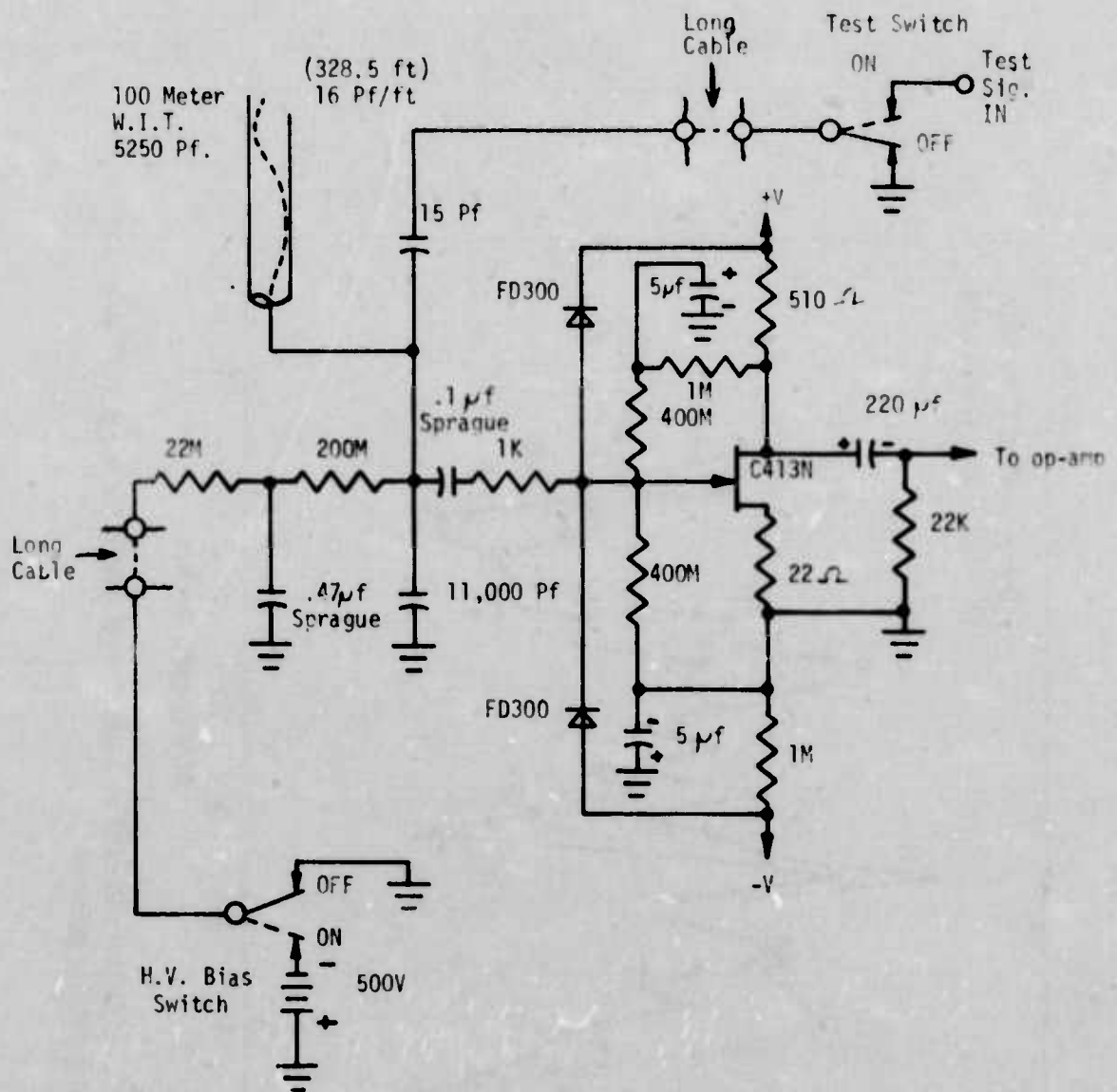


Figure 11 - Voltage bias provision in experimental WIT preamplifier.

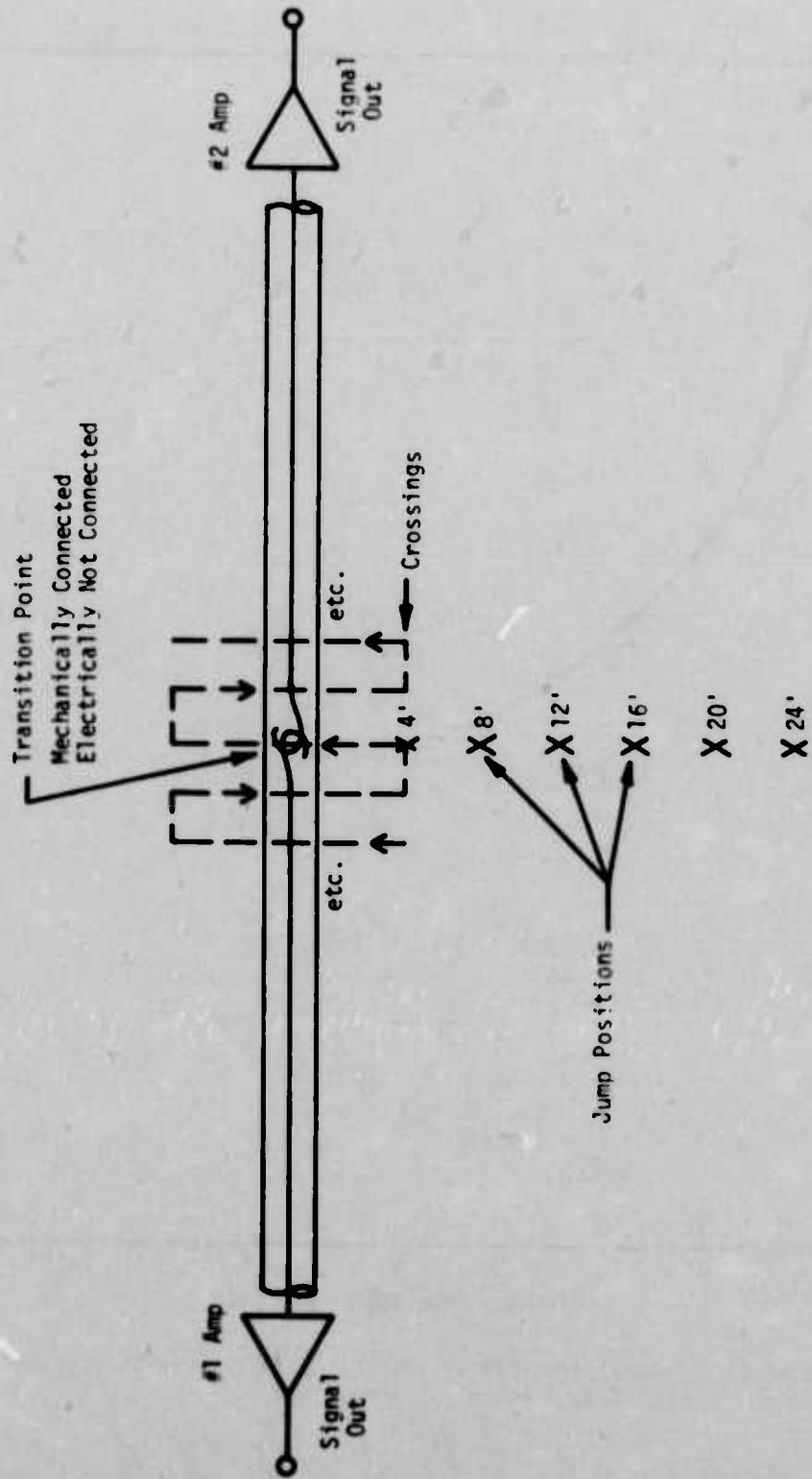


Figure 12 - Split sensor test setup.

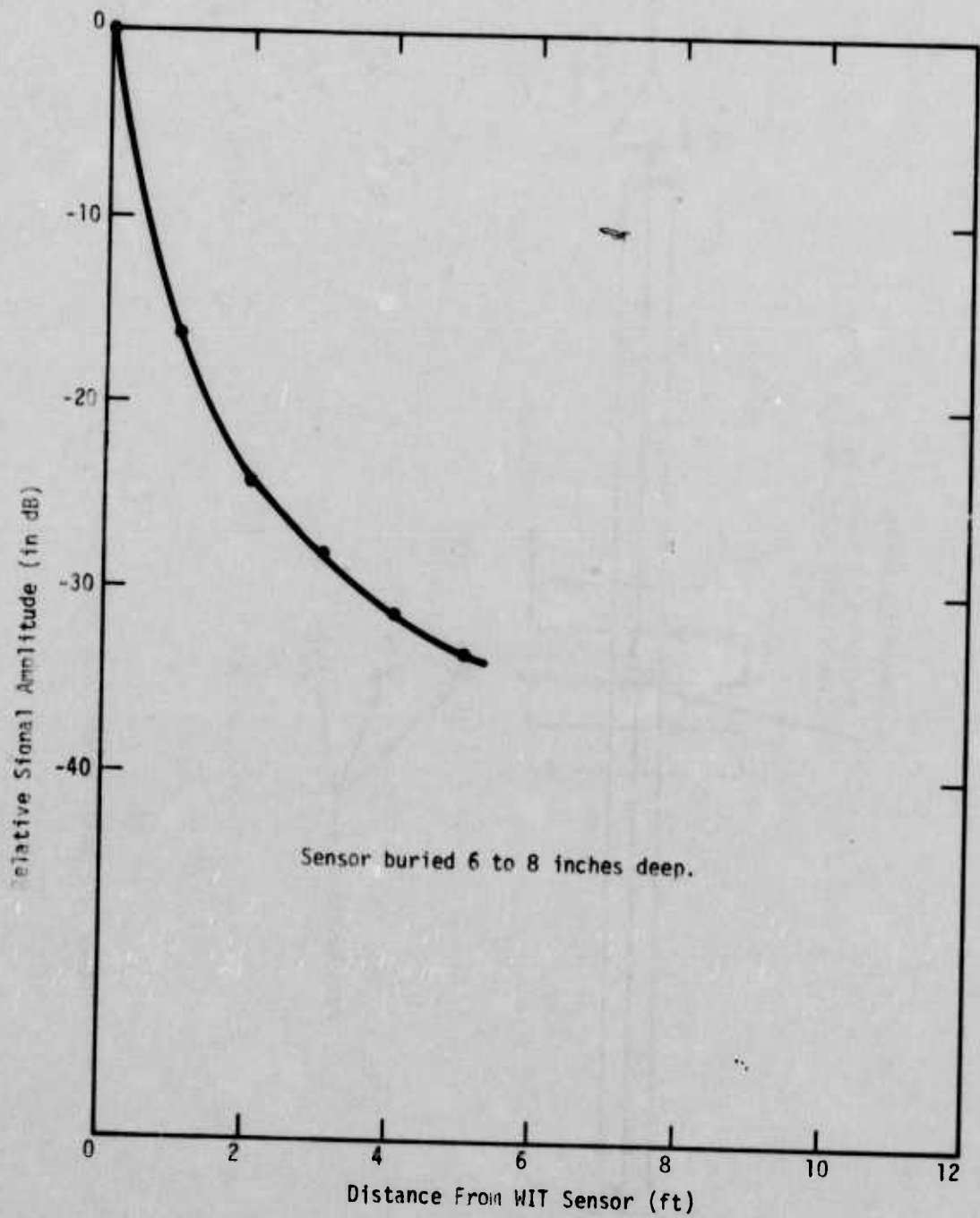


Figure 13 - Lateral sensitivity profile for WIT sensor, displacement mode (low frequency), ground wet.

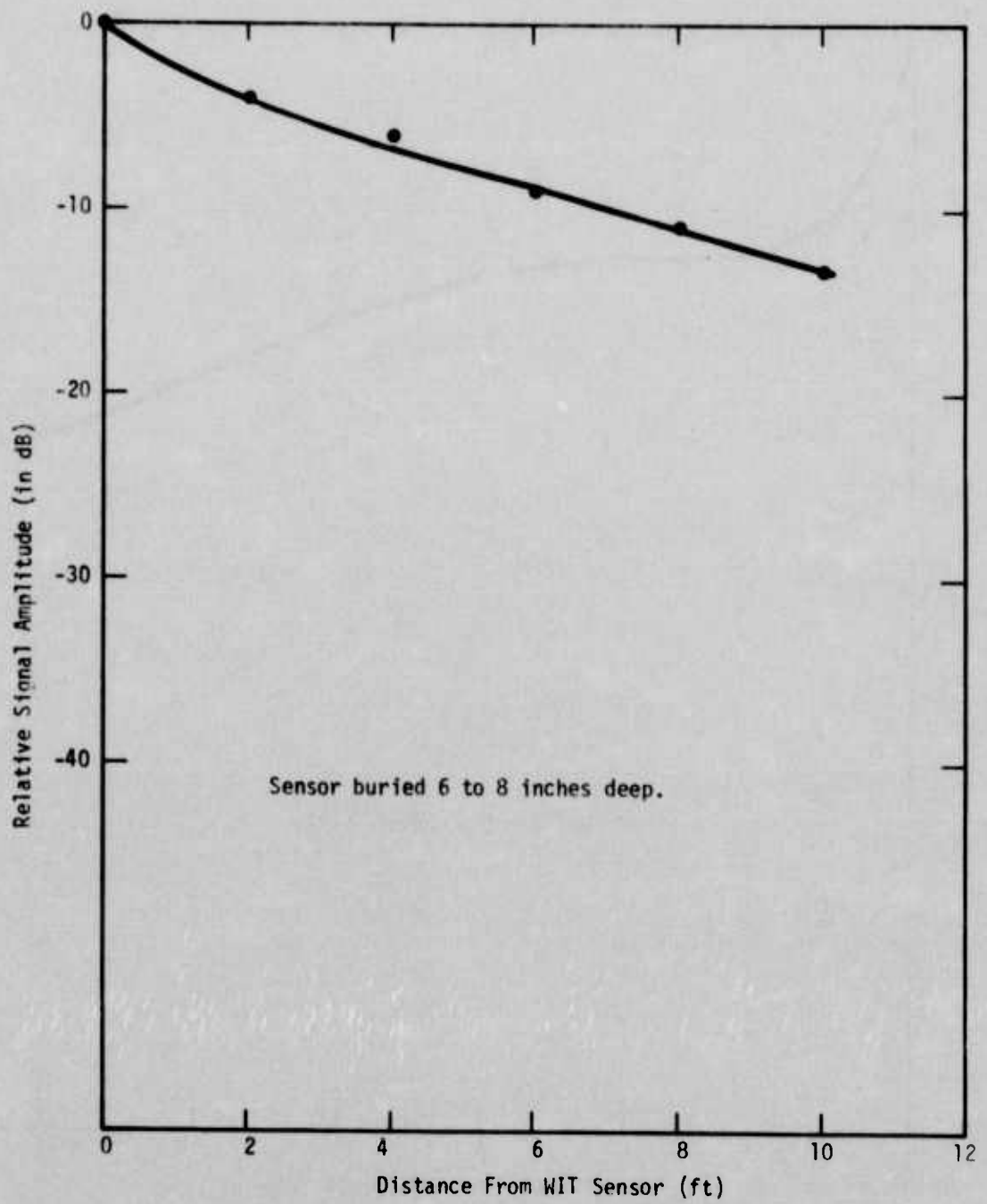


Figure 14 - Lateral sensitivity profile for WIT sensor, displacement mode (low frequency), ground frozen to 18" - 24" depth.

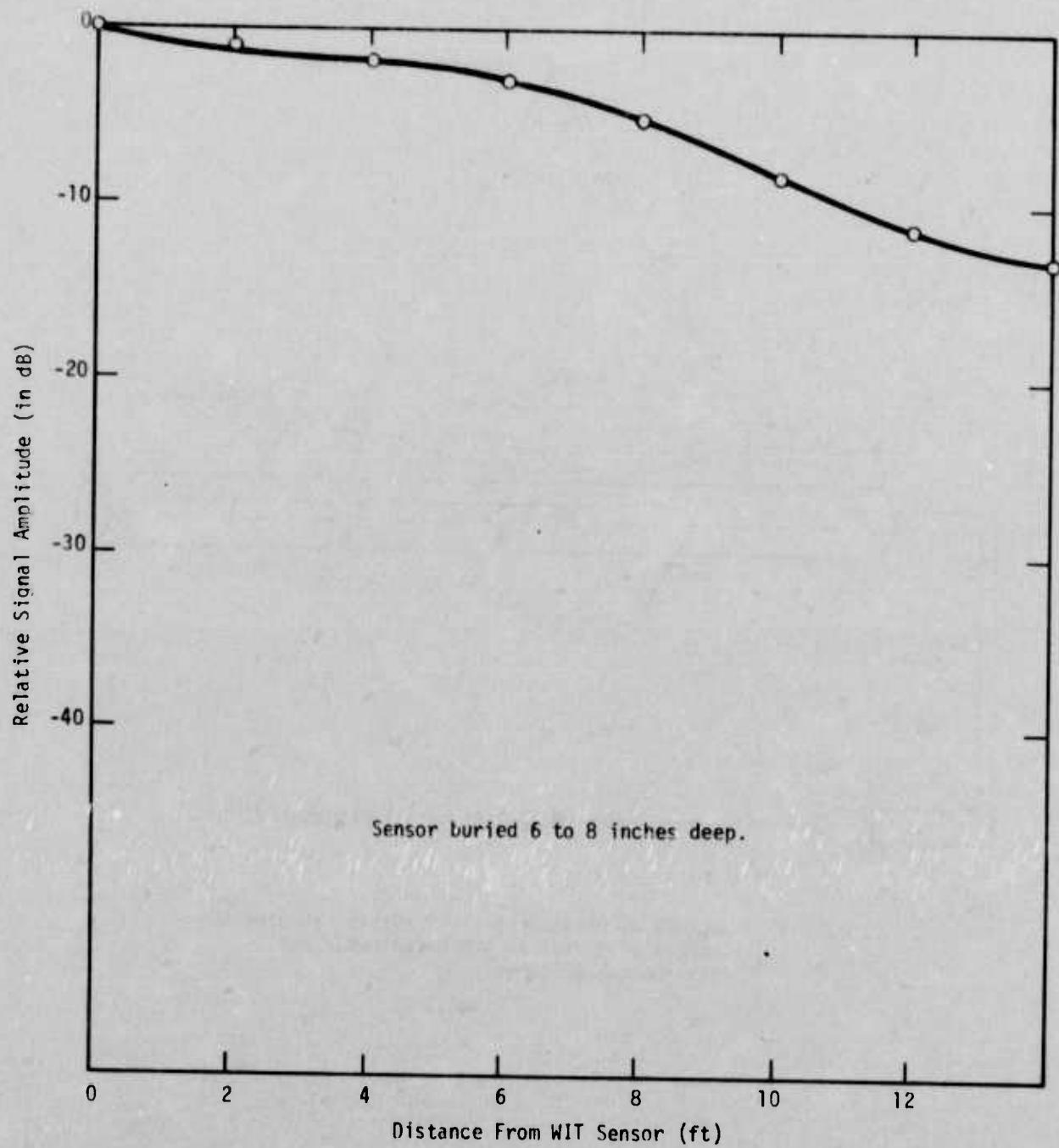


Figure 16 - Lateral sensitivity profile for WIT sensor, strumming mode (high frequency), ground frozen to 18" - 24" depth.

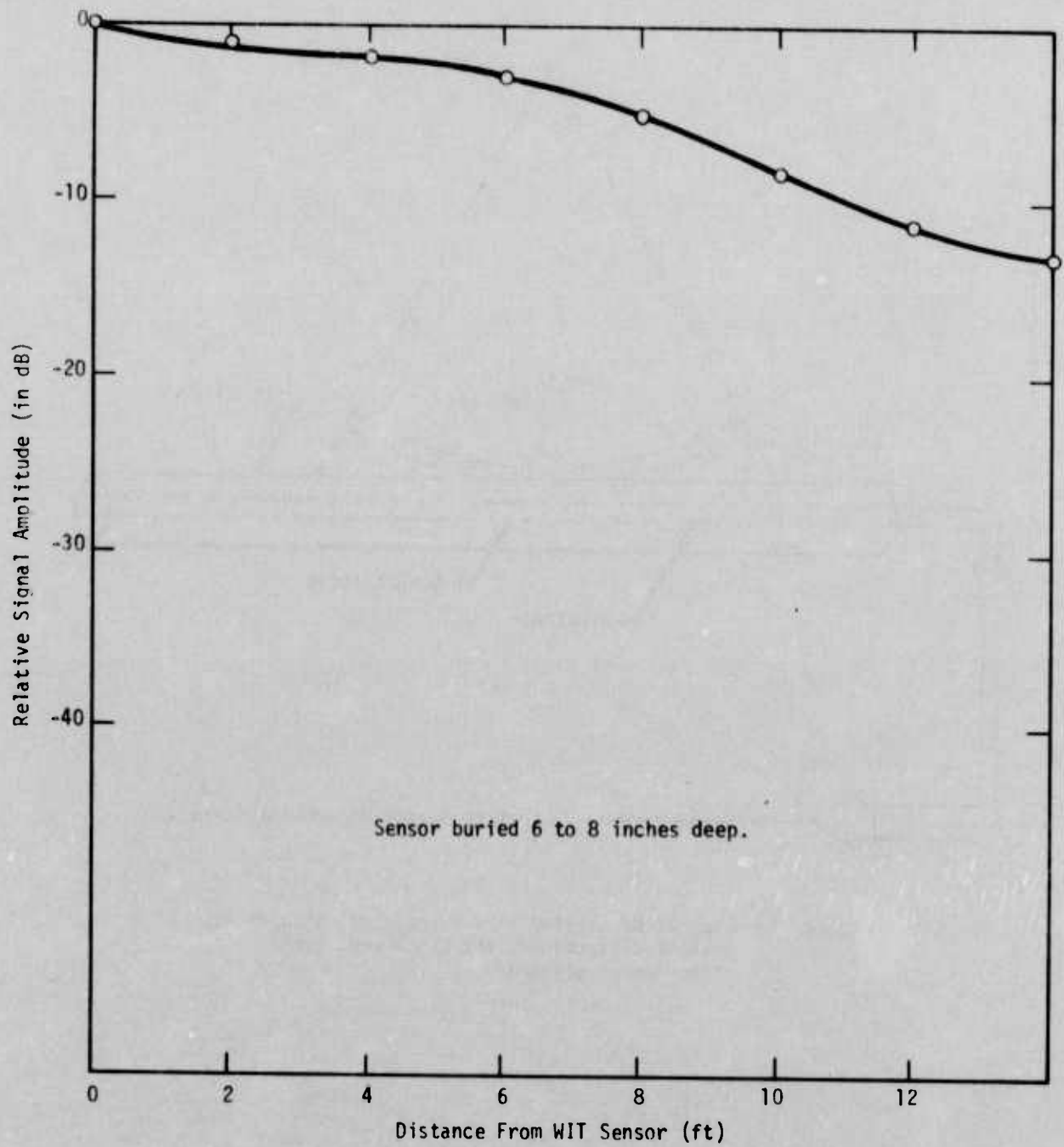


Figure 16 - Lateral sensitivity profile for WIT sensor, strumming mode (high frequency), ground frozen to 18" - 24" depth.

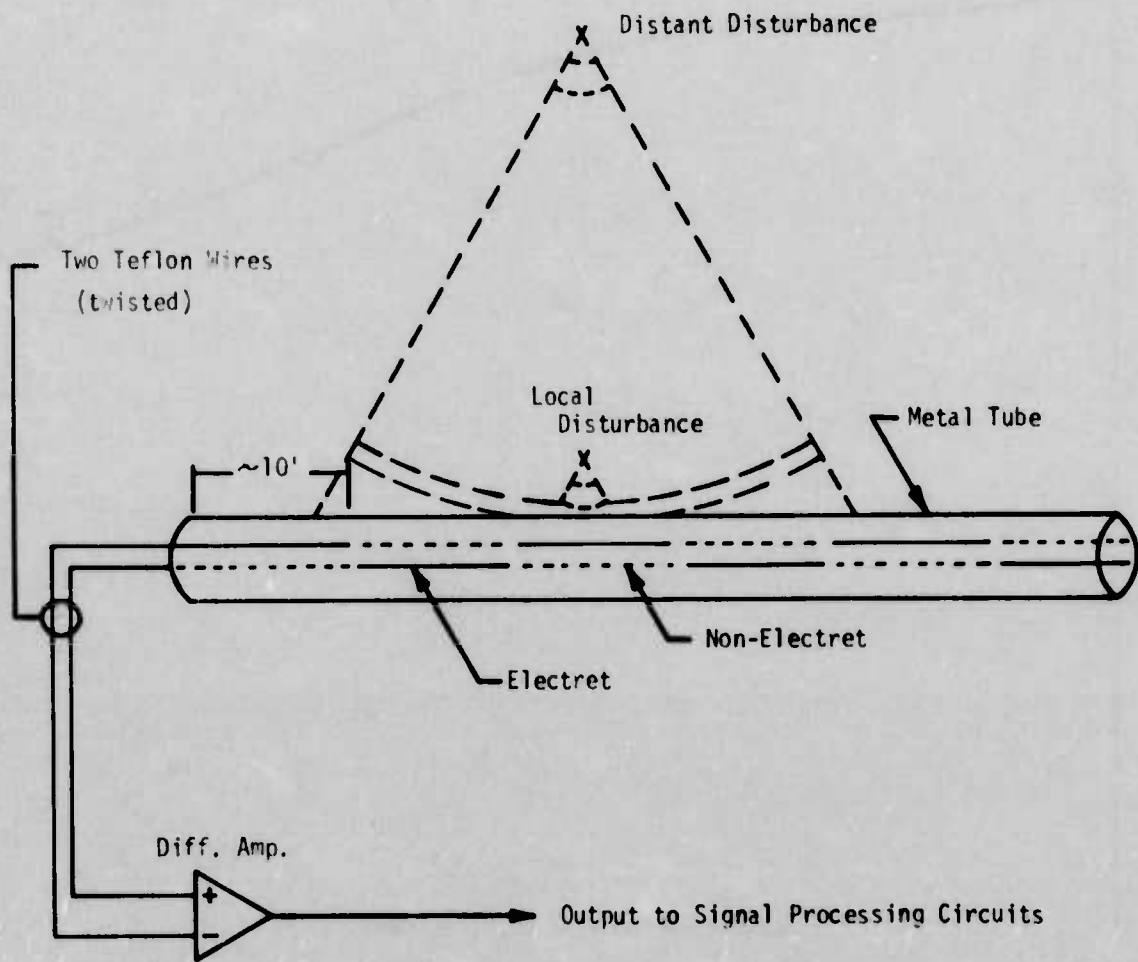


Figure 17 - Diagram of twisted wire WIT system, showing how distant disturbances are cancelled, local disturbances preserved.

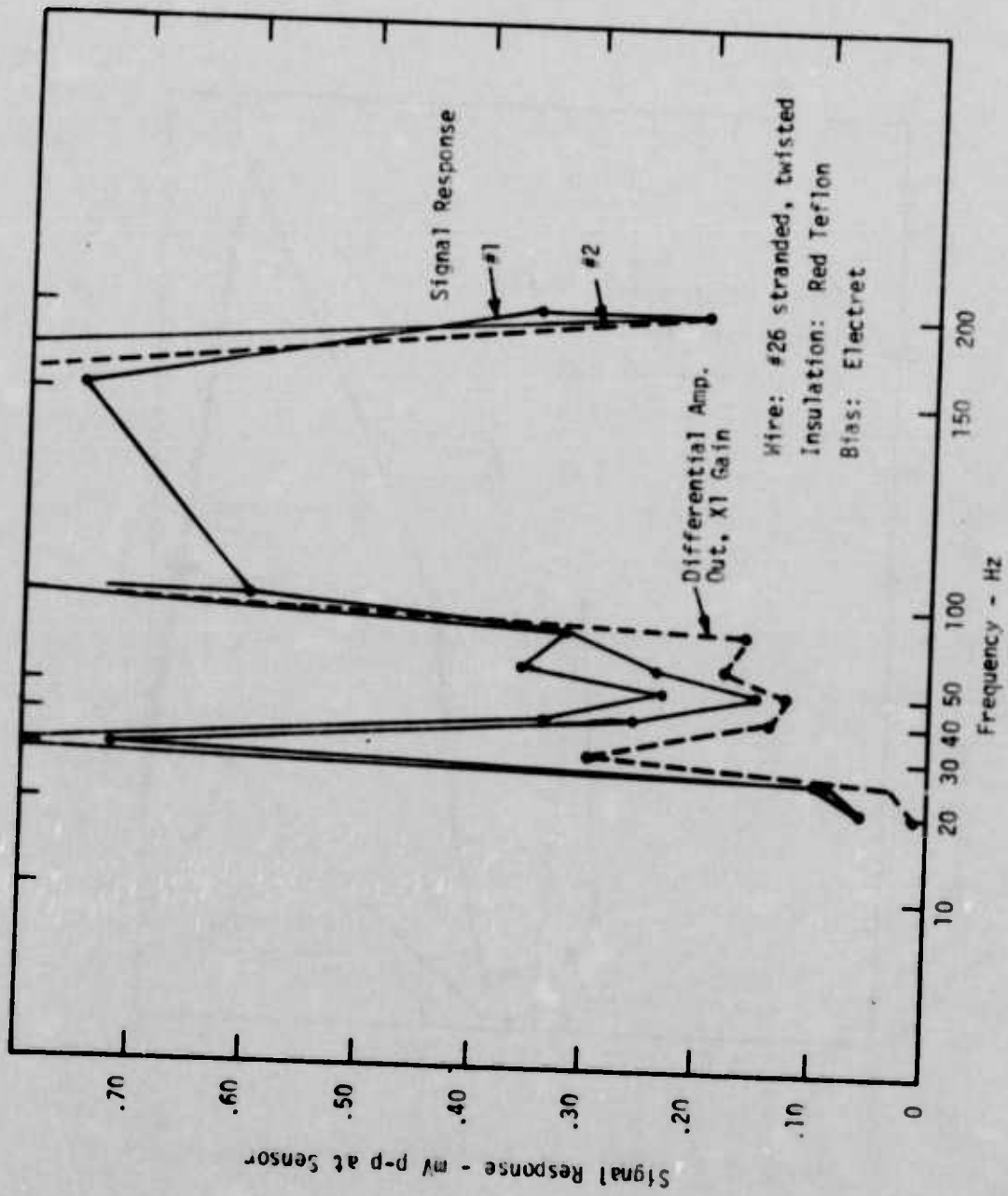


Figure 18 - Twisted pair cancellation test, electret wire.

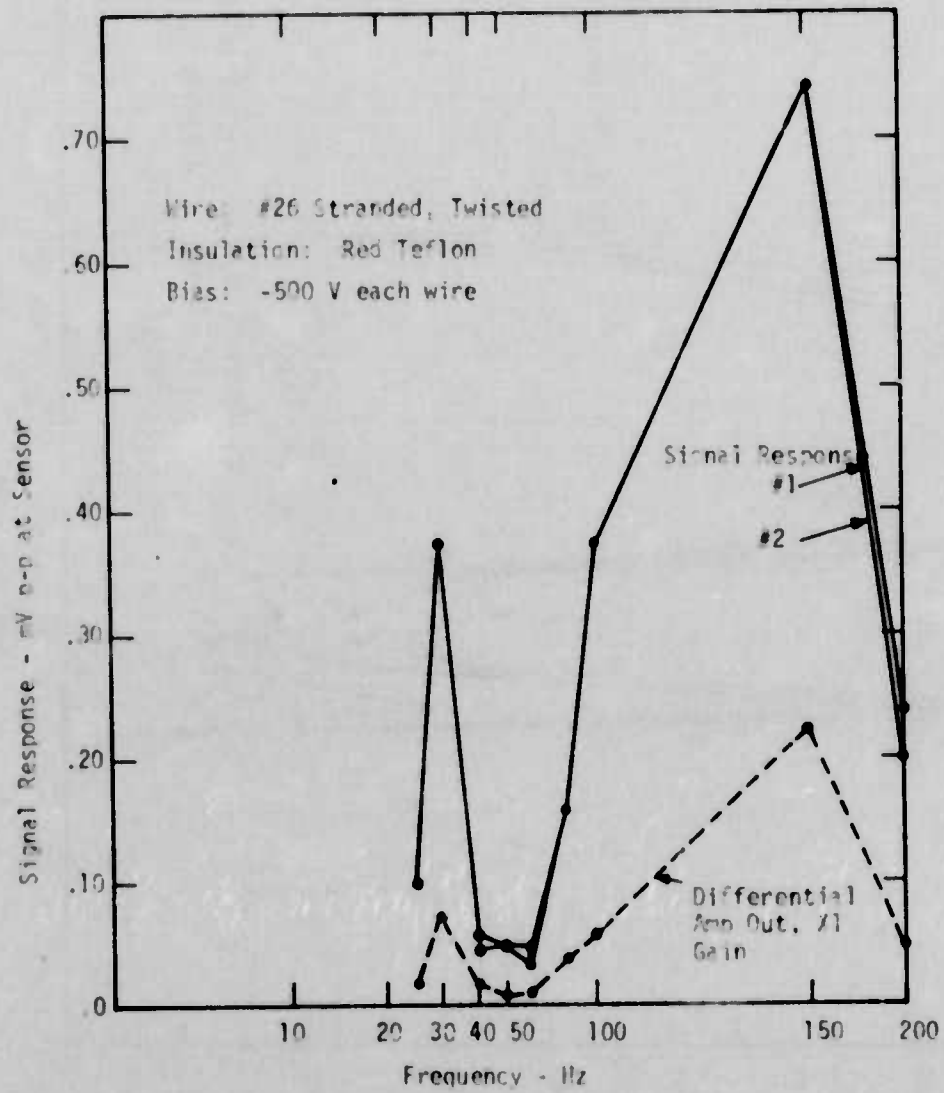


Figure 19 - Twisted pair cancellation test, biased wire.

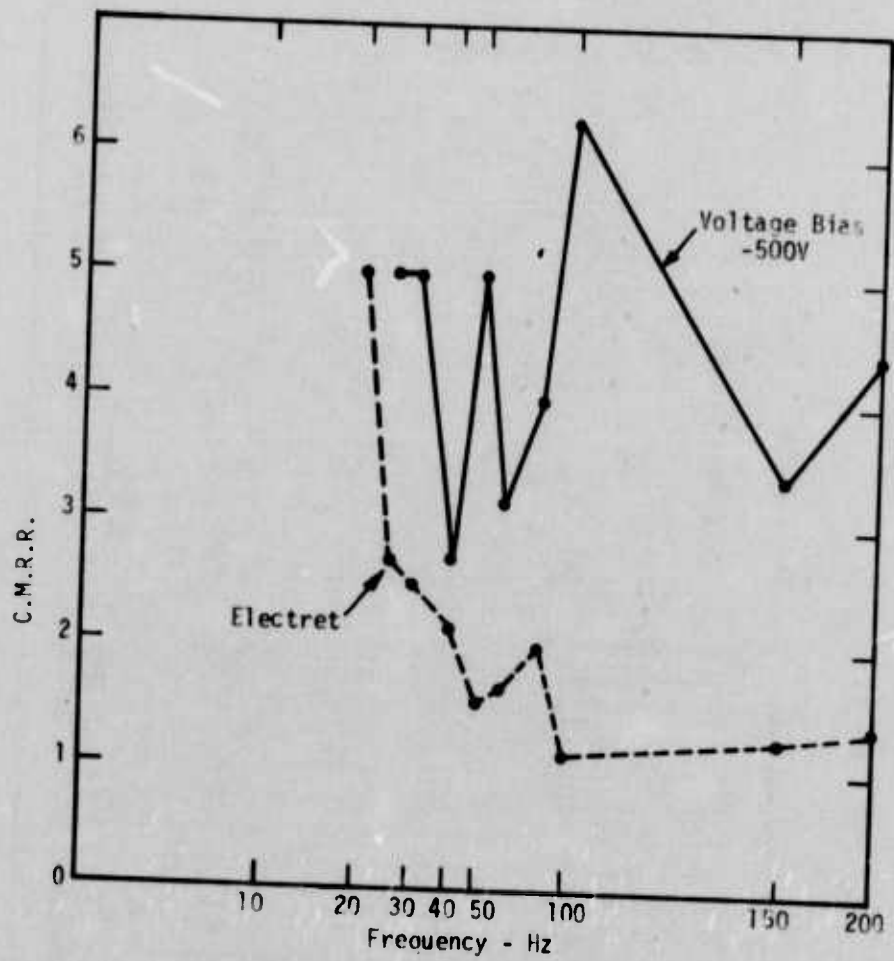


Figure 20 - Twisted pair cancellation. Comparison of common mode rejection ratios.

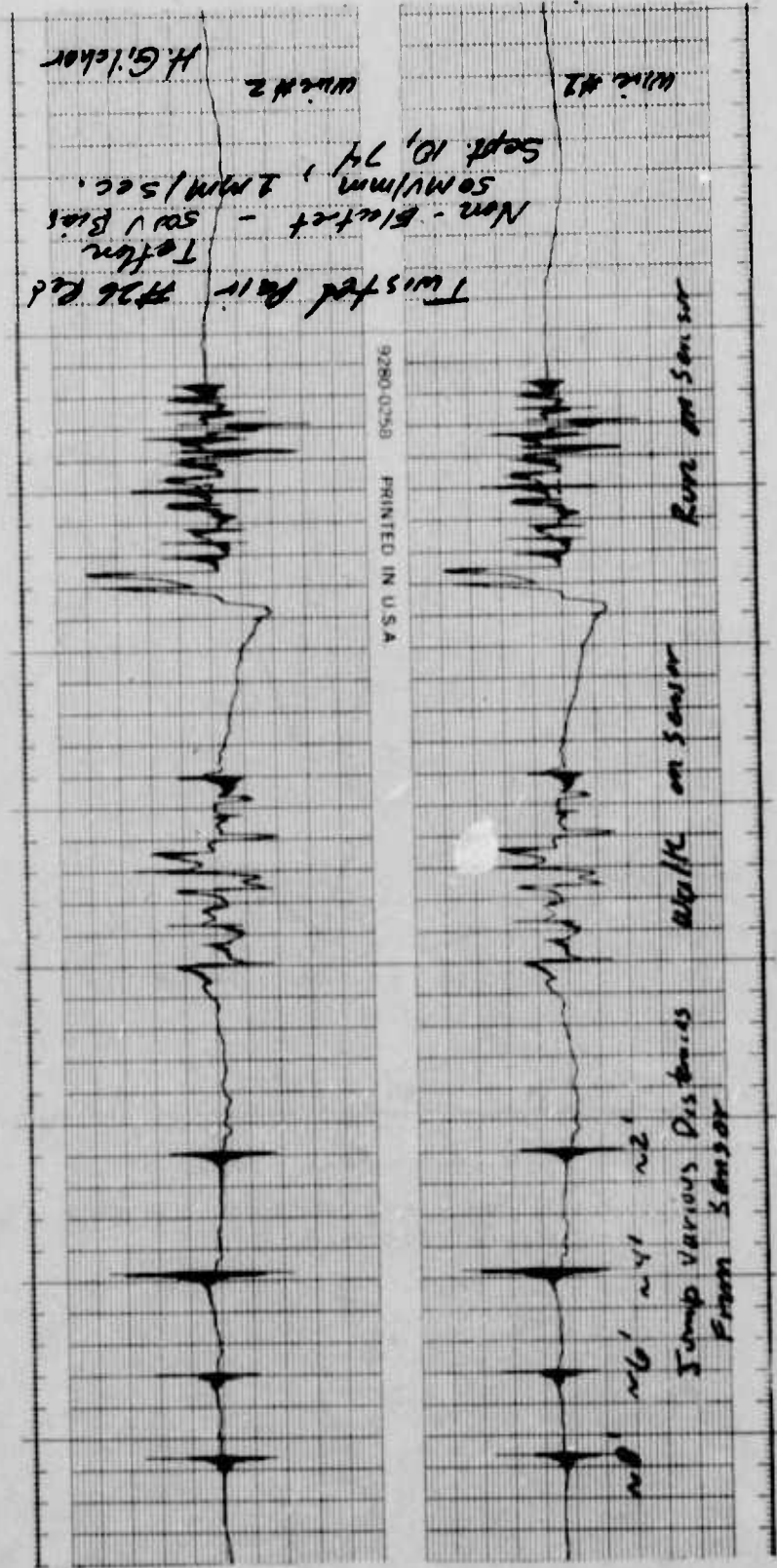


Figure 21 - Twisted pair outdoor test. Comparisons of individual wire signatures.

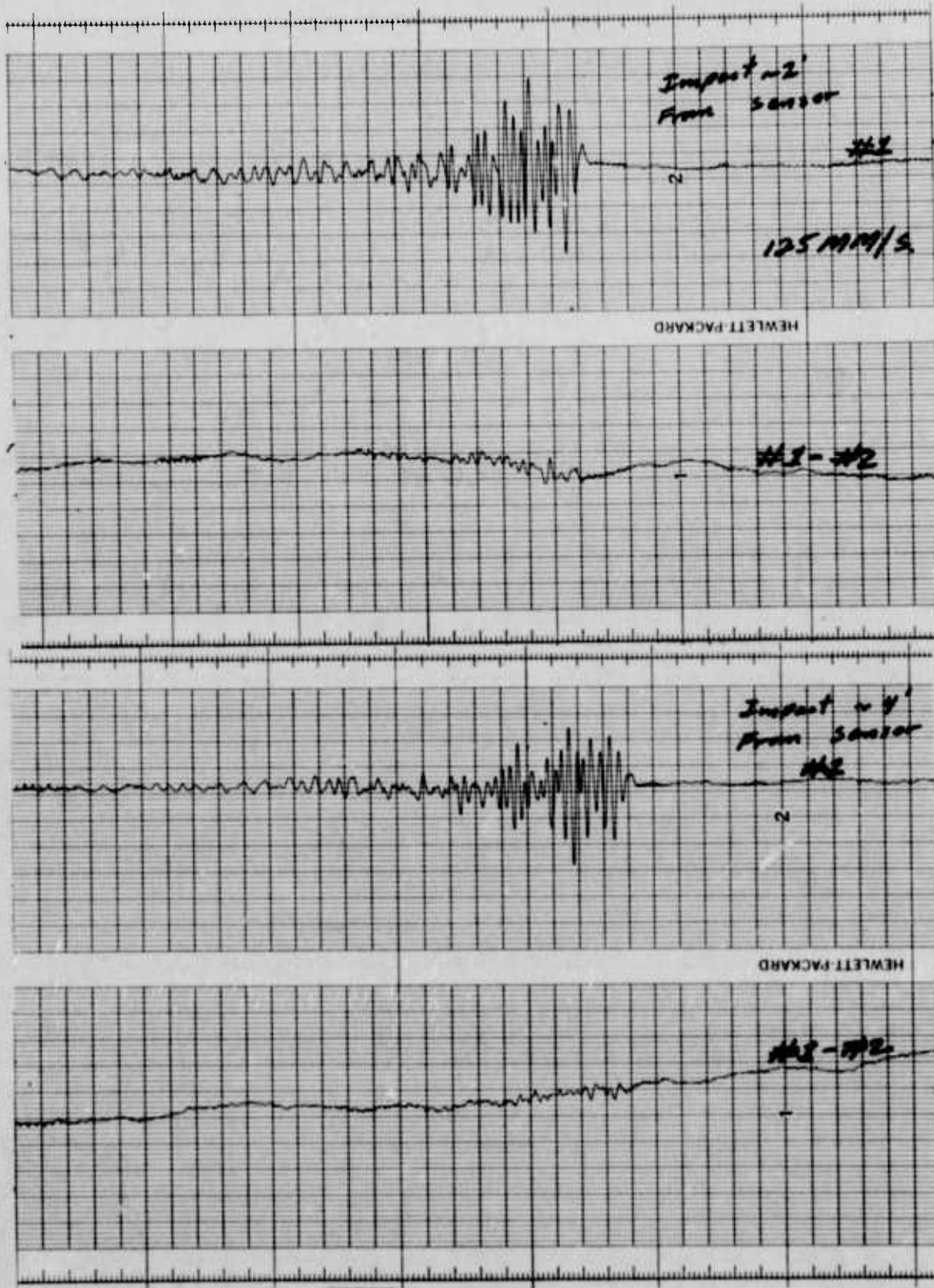


Figure 22 - Individually and differentially amplified impact signatures at two distances from sensor.

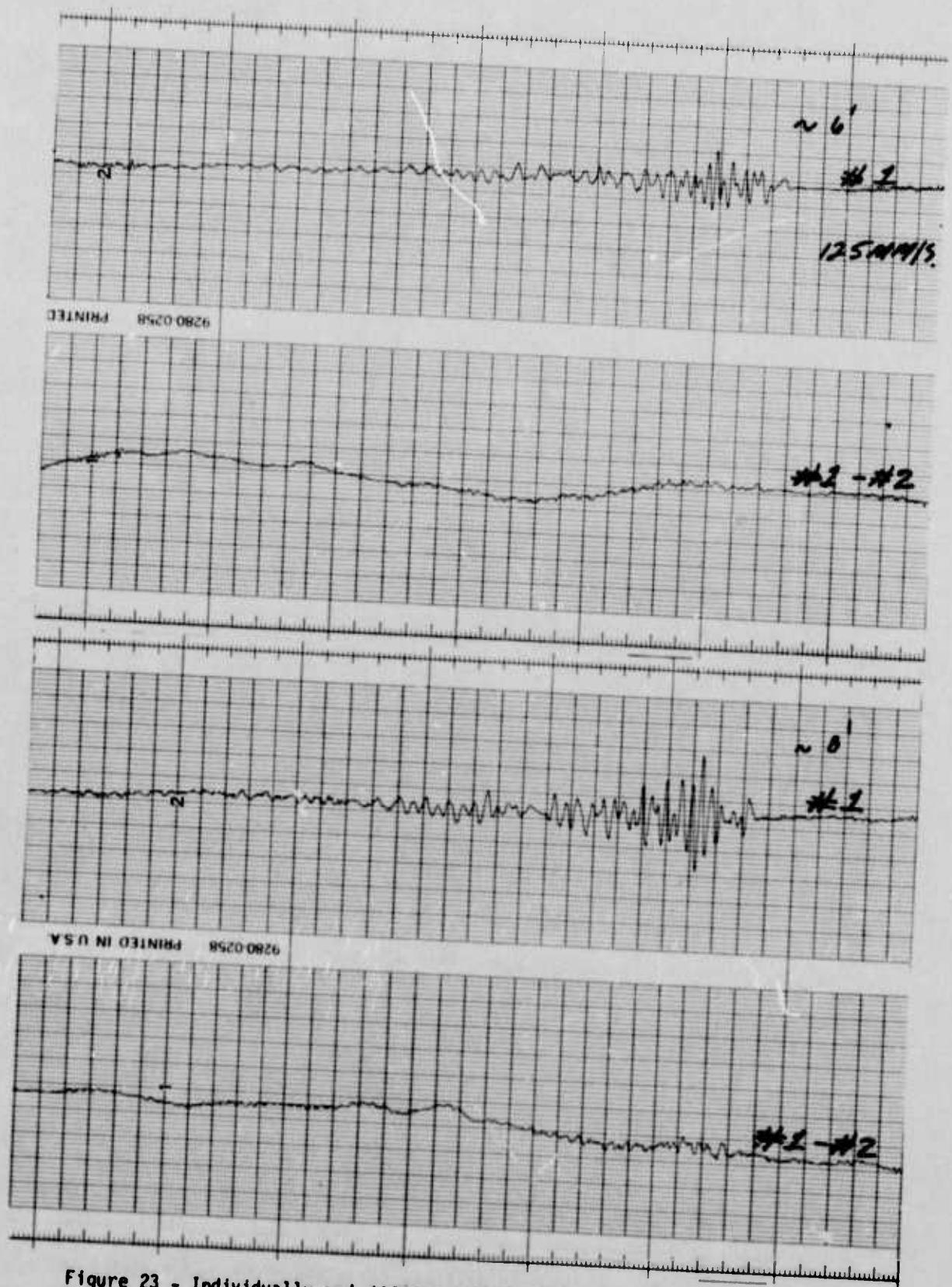


Figure 23 - Individually and differentially amplified impact signatures at two additional distances.

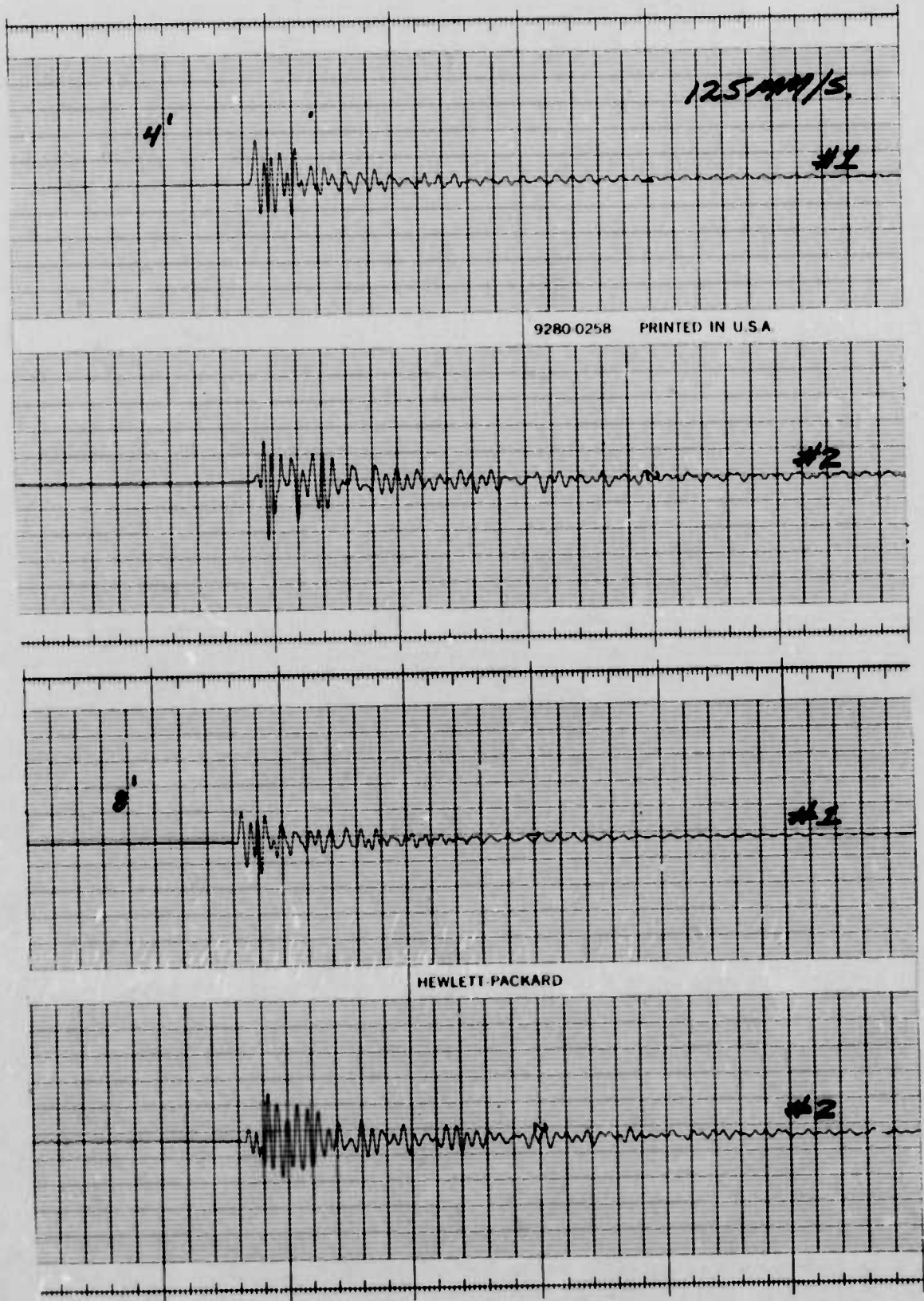


Figure 24 - Individual wire signatures for impact disturbances at 4' and 8' using sensor configuration of Figure 12.

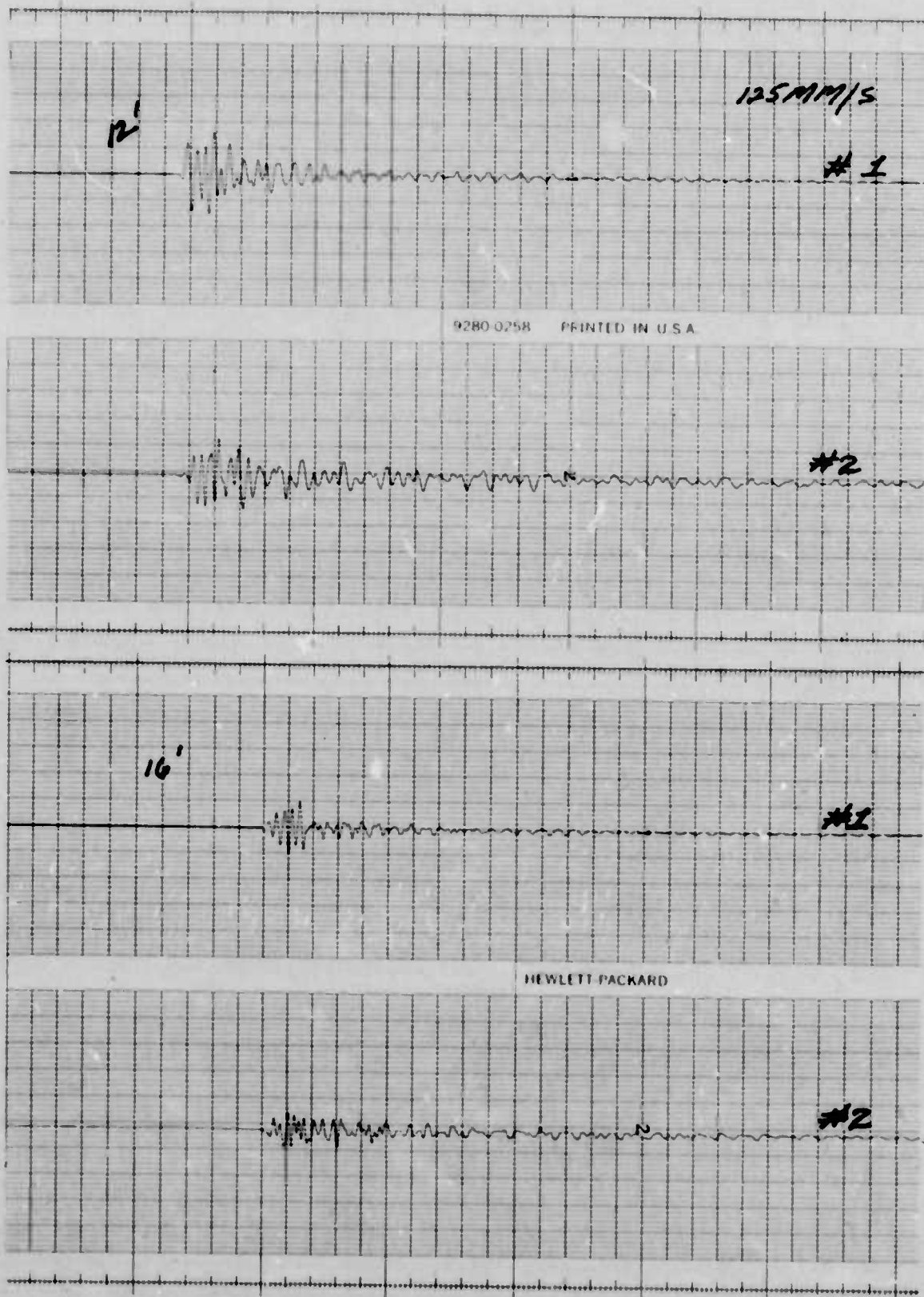
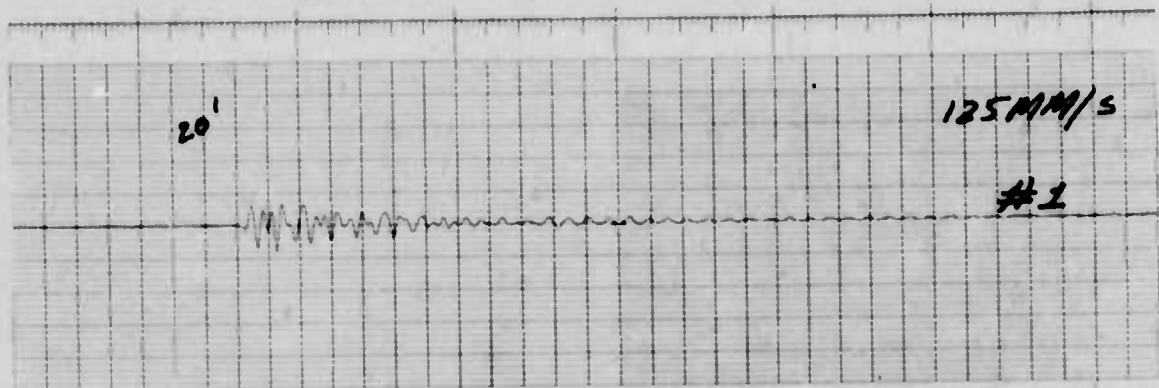
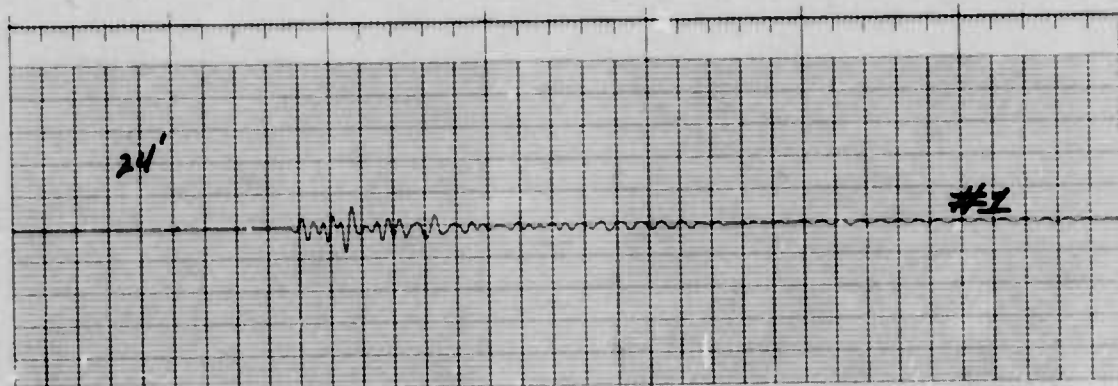
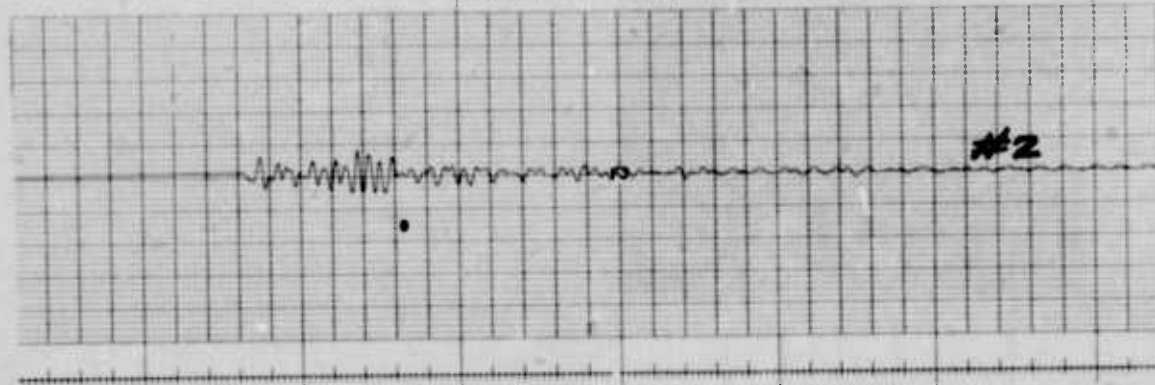


Figure 25 - Individual wire signatures for impact disturbances at 12' and 16' using sensor configuration of Figure 12.



9280 0258 PRINTED IN U.S.A.



9280 0258 PRINTED IN U.S.A.

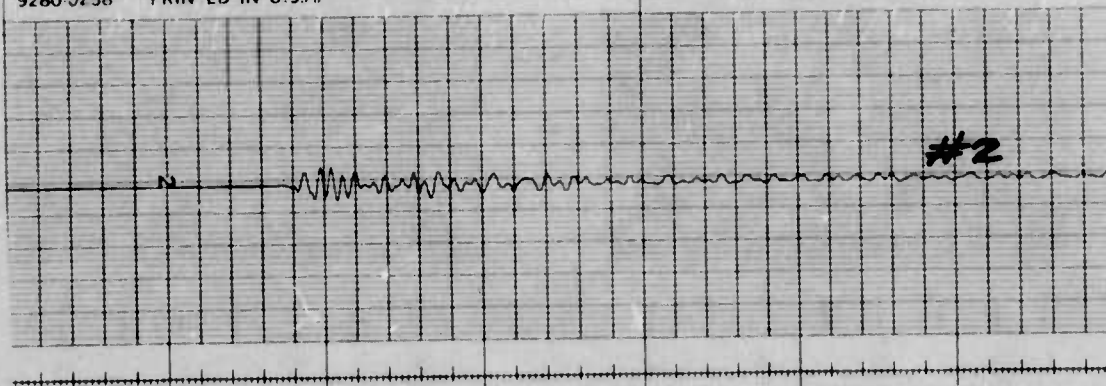
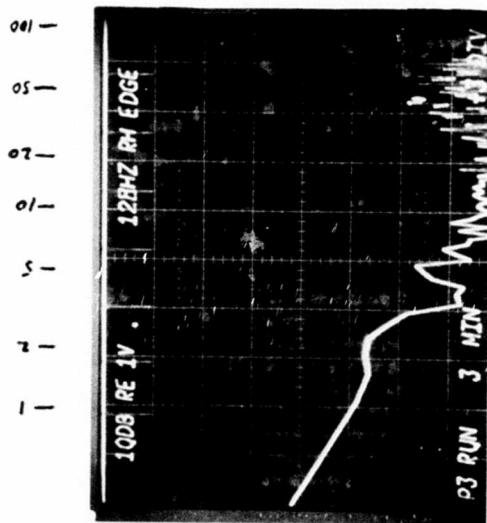
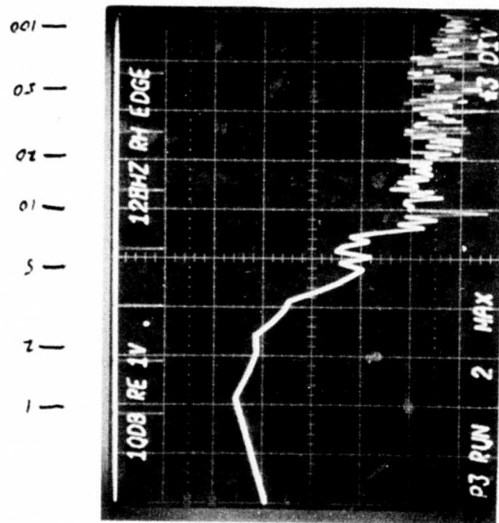
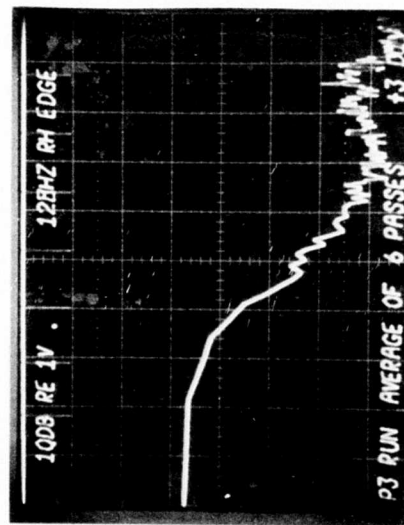


Figure 26 - Individual wire signatures for impact disturbances at 20' and 24' using sensor configuration of Figure 12.

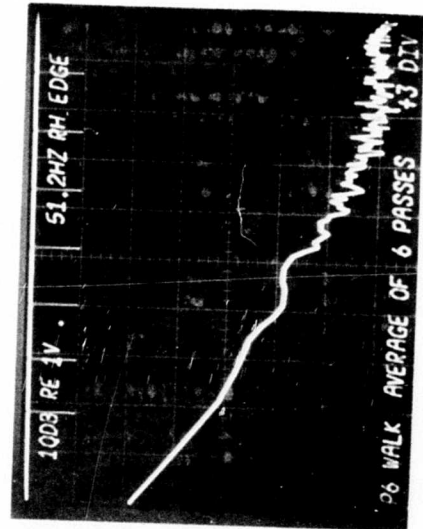
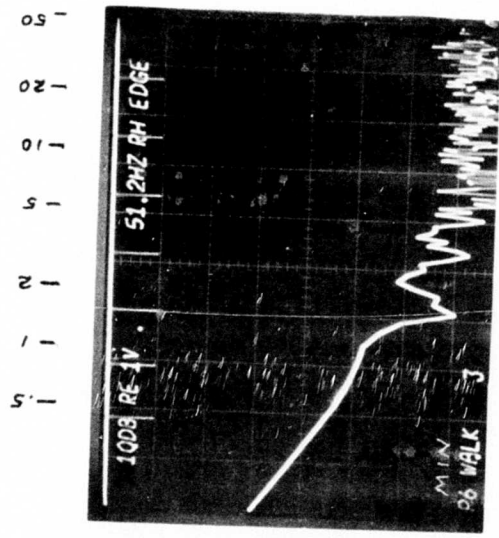
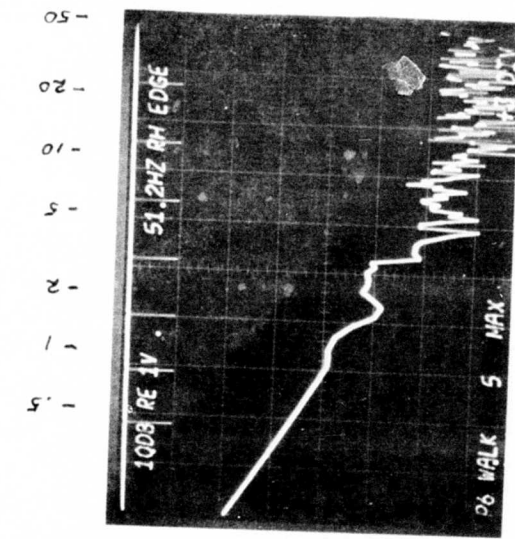


0 dB
-20
-40
-60



0 dB
-20
-40
-60

Figure 27 - Run intrusions, 60°F, ground damp.
50 dB total amp gain.



0dB -

-20 -

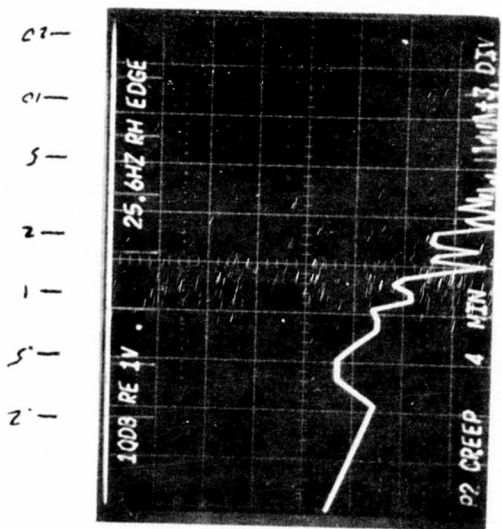
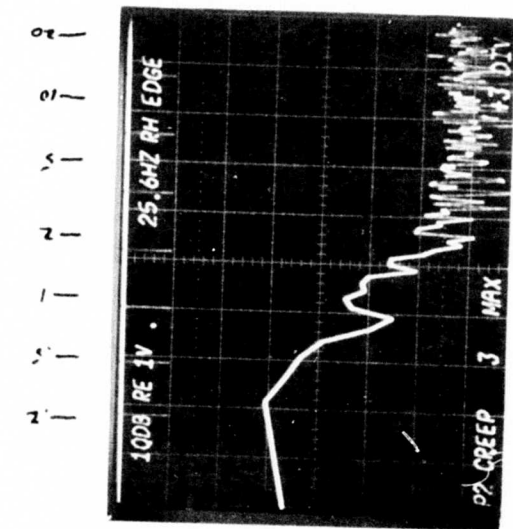
-40 -

0dB -

-20 -

-40 -

Figure 28 - Walk intrusions, 60°F, ground damp. 50 dB total amp gain.



0 dB -
 -20 -
 -40 -
 -60 -

0 dB -
 -20 -
 -40 -
 -60 -

Figure 29 - Creep intrusions, 60°F, ground damp. 50 dB total amp gain.

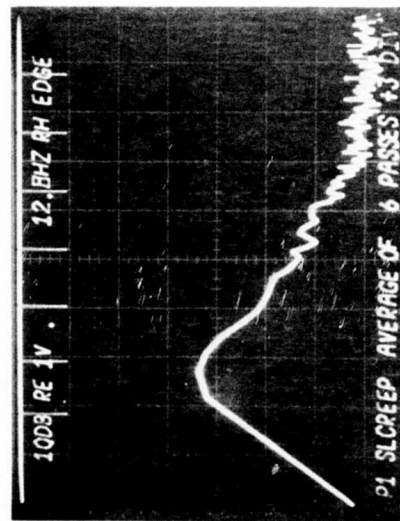
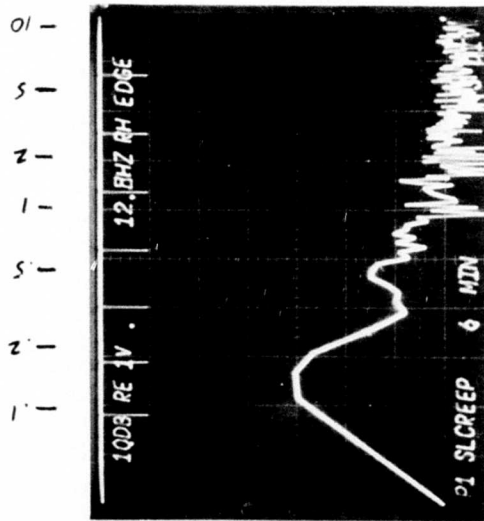
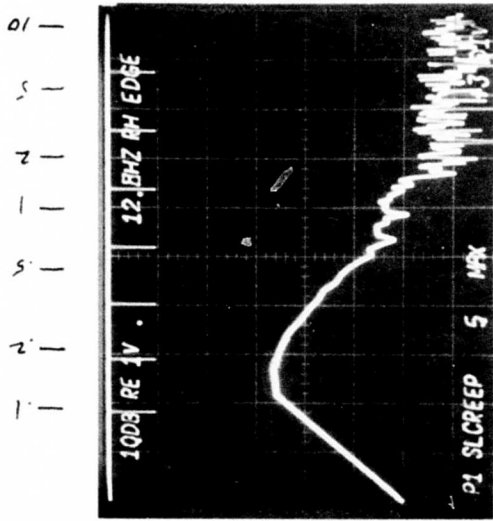
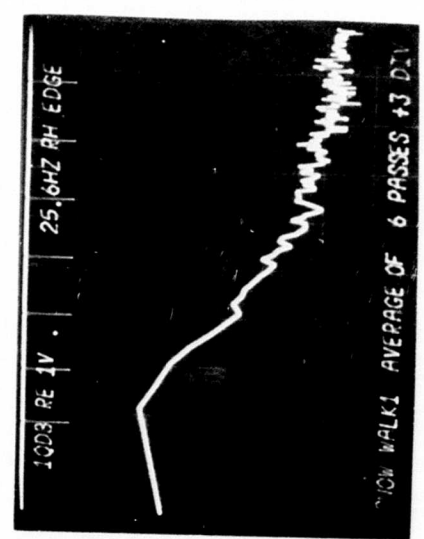
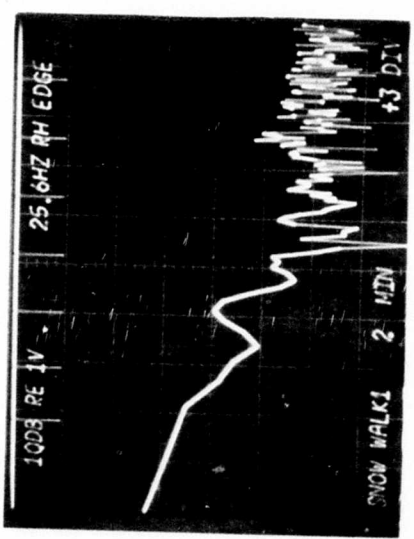
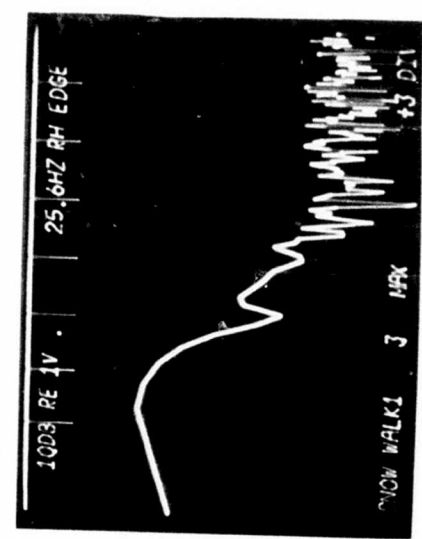


Figure 30 - Slow creep intrusions, 60°F, ground damp. 50 dB total amp gain.



0 dB —
 -20 —
 -40 —
 -60 —

0 dB —
 -20 —
 -40 —
 -60 —

Figure 31 - Snow walk intrusions, 33°F, 5" wet snow. 60 dB total amp gain.

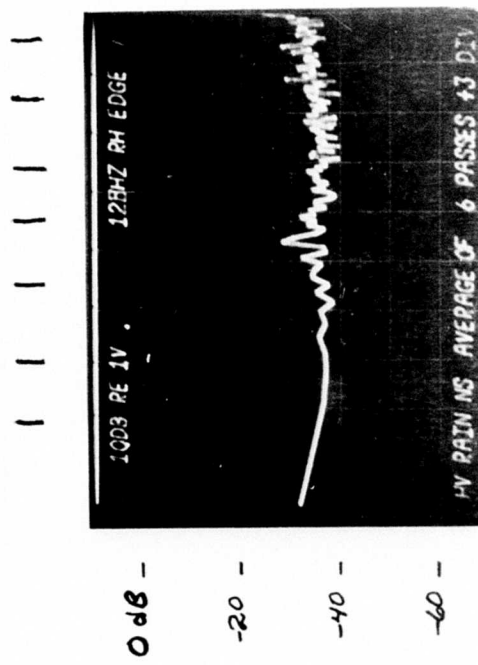
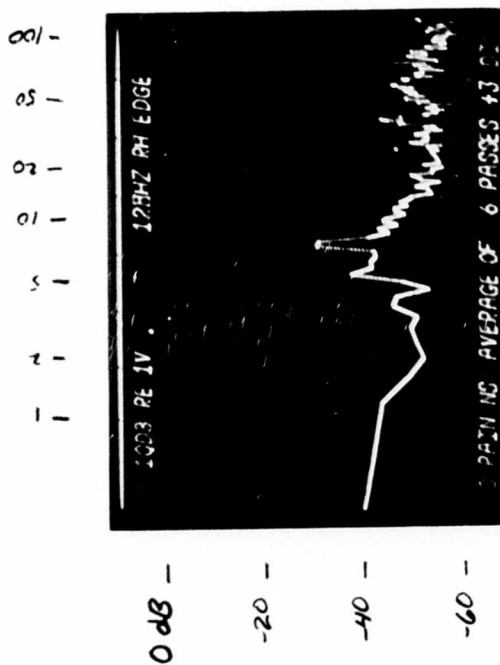
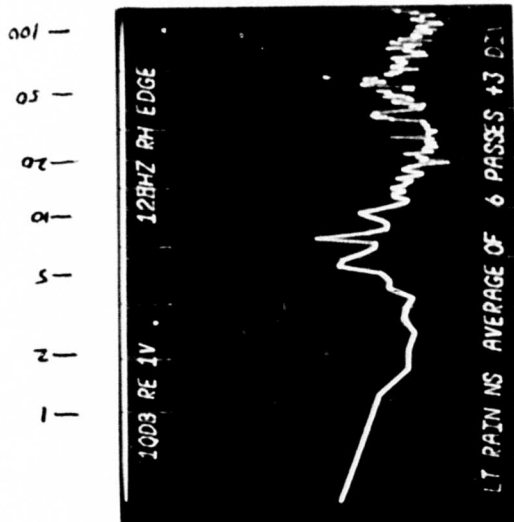


Figure 32 - System background noise, light rain, heavy rain. 80 dB total amp gain.

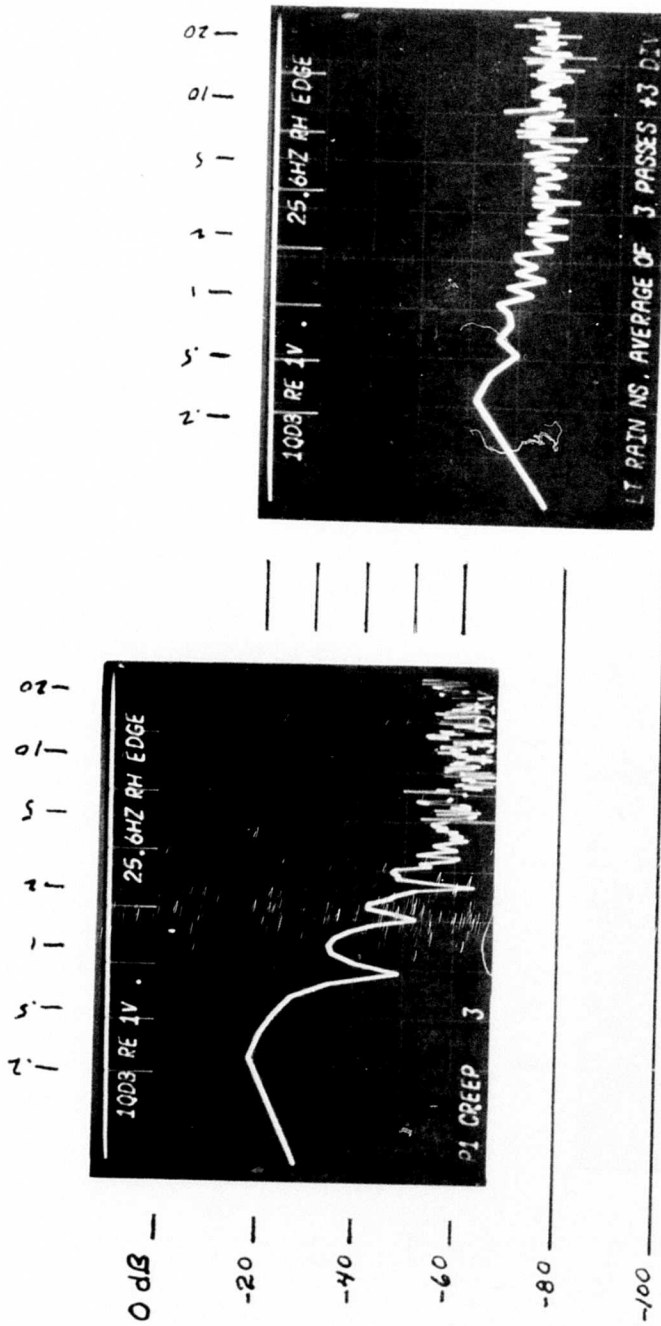
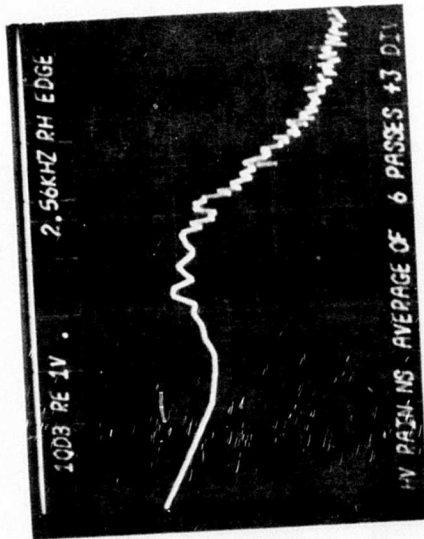
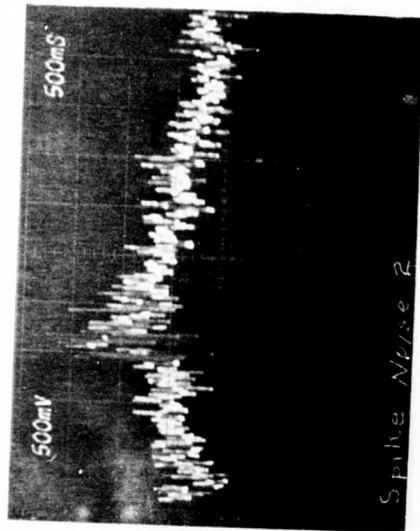
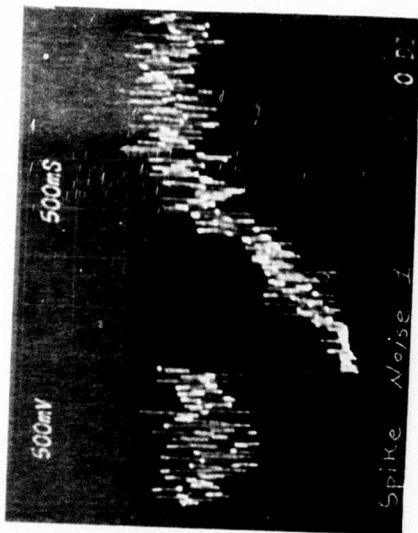


Figure 33 - Creep intrusions compared to light rain noise. Intrusions at 50 dB gain, noise at 80 dB gain.



0 dB —
 -20 —
 -40 —
 -60 —

Figure 34 - Wideband sensor response, heavy rain. 80 dB total amp gain.



58

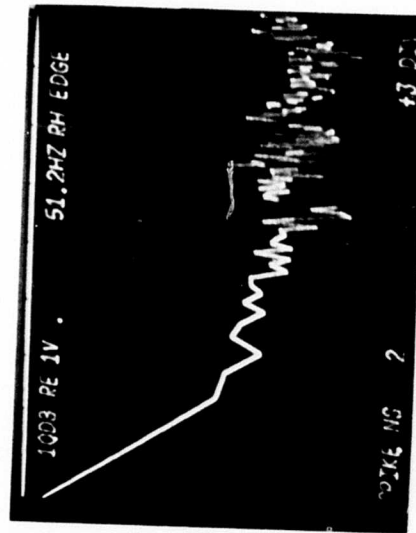
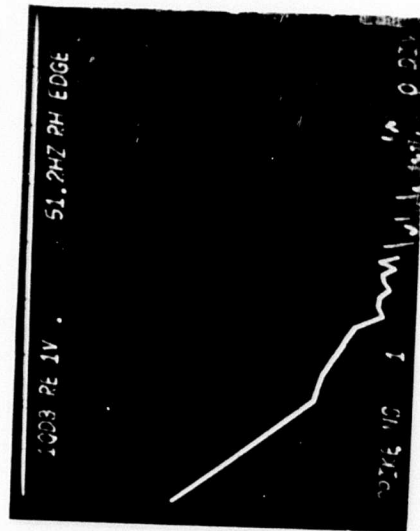


Figure 35 - Spike noise. 80 dB total amp gain.

APPENDIX A

INSTRUCTION MANUAL FOR R.A.D.C. INSTALLED EQUIPMENT

Line Sensor

The line sensor is fabricated with 1/4 inch O.D. copper refrigerator tubing covered by a plastic insulating material. The electret is made up of #26 red T.F.E. teflon flex hook-up wire, which is a natural electret. The wire is pulled into the tube enclosure and the tube is purged with dry nitrogen to eliminate moisture. Both ends are immediately sealed, the preamplifier end being provided with a vacuum feed-through seal which is connected to the wire and acts as a connector. The WIT sensor is connected to its preamplifier with an ordinary swage lock tubing fitting which acts as a mechanical connector and a seal.

Preamplifier

The preamplifier, which is directly connected to and buried with the WIT sensor, is housed in a sealed stainless steel, cylindrical shaped container. A sensor cable female connection is welded to the end of this housing. At the opposite end is a removable lid with an "O" ring seal. This lid has a permanently sealed multiconductor cable fed through to permit the required power and signal lines access to the preamplifier board.

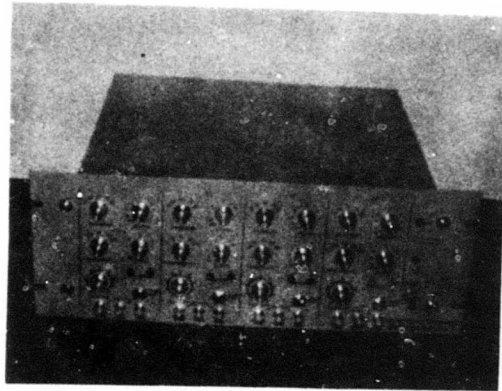
The 40 dB preamplifier circuit as shown in Figure A1, is built up on a single glass epoxy circuit board. Transistor Q1 and associated circuit components make up a 20 dB amplification stage. This P.E.T. transistor has very good low noise characteristics in addition to its high input impedance. The amplifier input is connected to a 100 meter

WIT sensor which has an approximate capacitance of 4800 pF. Capacitor C3 in parallel with the sensor has a total of about .016 μ F capacitance. The D.C. input impedance of the amplifier is 250 M Ω and in parallel with .016 μ F input capacitance, results in a low frequency cutoff of a little less than .05 Hz. The test signal, which is for the purpose of testing the complete system, is connected to the amplifier front end through capacitor C1. The test signal is attenuated 60 dB as a result of the voltage divider action of C1 and the parallel combination of the sensor capacitance and C3. Component E1 is a high voltage transient arrester. Low noise, low leakage diodes D1 and D2 in combination with R1 provide additional high voltage protection to transistor Q1. Resistor R2 provides D.C. feedback to provide for unity gain at D.C. and, as a result, good bias stability. Capacitor C4 shorts the feedback signal to ground over the operating frequency range. The output from the drain is coupled to a UA741 operational amplifier which provides an additional 20 dB of gain and a low drive impedance. Two stages of decoupling are provided on both the +15 V and the -15 V bus voltages. Both power inputs and the signal output are provided with high voltage transient suppressors, E2, E3, and E4, for lightning protection. Additional protection is provided on the power buses by resistors R10 and R14 and associated zener diodes D5 and D8. The signal output has additional transient protection provided consisting of R15 and C12 and zener diodes D6 and D7. The maximum output voltage swing is about 15 V p-p. The preamplifier band pass frequency ranges from .05 Hz to about 9 kHz; the overall voltage gain is 40 dB.

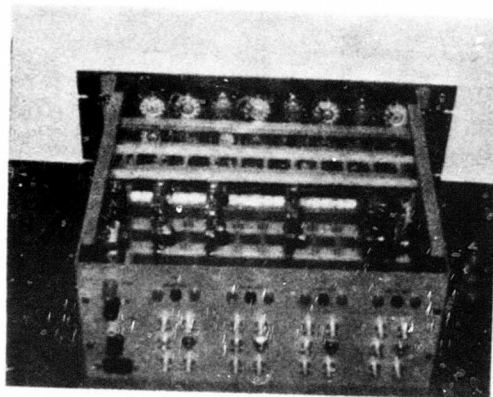
Console Functional

The instrument console for the four WIT sensor systems, as shown in Figure A2(photo), was designed for maximum operator freedom in selecting test parameters.

The front panel is divided into four separate sections, one for each sensor. Each of the four sections has the functions shown in Figure A3. The input from a preamplifier is fed into the broadband



Front



Rear

Figure A2 - Front and rear view of completed console.

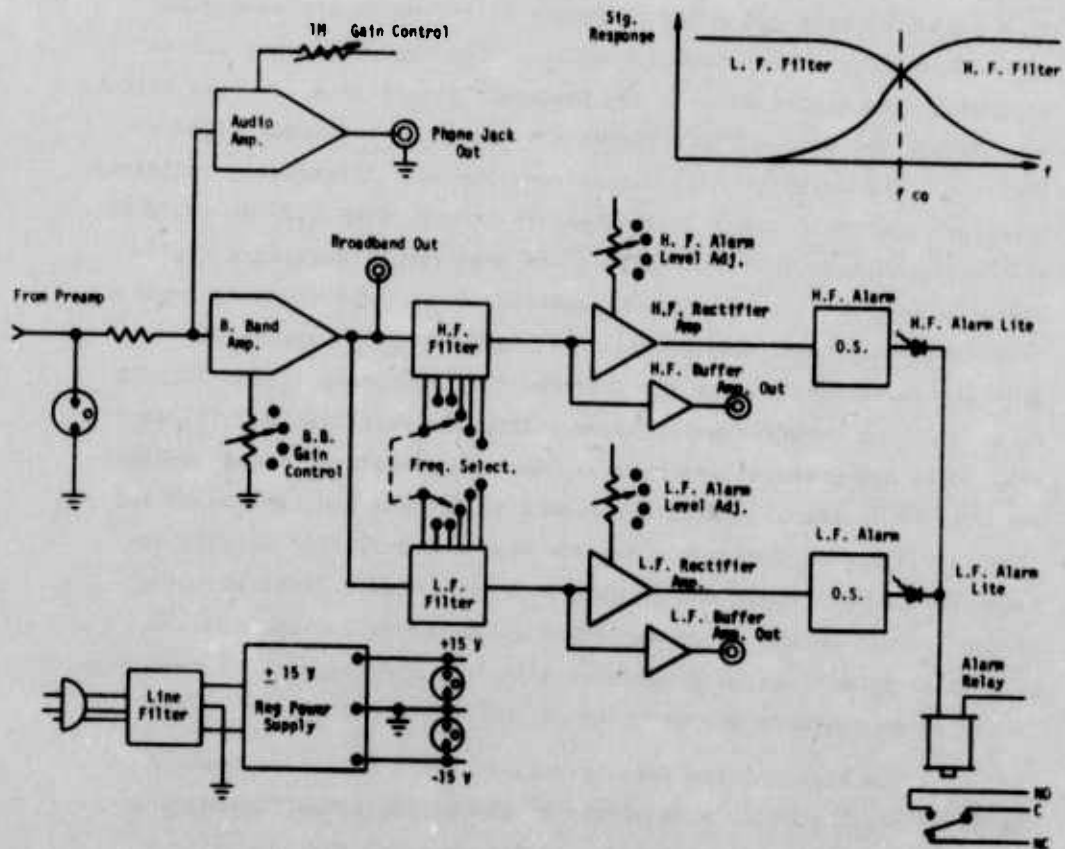


Figure A3 - Block diagram of console, one channel.

amplifier. A front panel gain selector switch provides total system gain selection in the range of 40-80 dB. The broadband amplifier bandwidth ranges from .05 Hz to 10 kHz. The amplifier output is fed to a high frequency and a low frequency filter which are controlled by a single front panel selector switch. The high frequency filter is a high pass filter and the low frequency filter is a low pass filter, both having the same cutoff frequency as shown on the upper right of Figure 3. The selector switch provides five cutoff frequency positions. These are spaced at one octave intervals ranging from 1.25 Hz to 20 Hz. The output signals from the filters are each fed to rectifier amplifiers which convert positive and negative signal excursions to negative excursions only, and also provide low impedance drive capability. Separate buffer amplifiers are provided for monitoring filter outputs directly. The negative going signals from the rectifier amplifiers are fed to one shot-multivibrators. When the negative signal amplitude exceeds -10 V, the appropriate one-shot is tripped and remains on for about a 0.5 second duration. The one shot multivibrator outputs are connected in "or" logic and actuate an alarm relay. Light emitting diodes located on the front panel are connected in series with the multivibrator outputs to provide visual alarm indications. Connections to the relay contacts are provided on the back panel of the console.

The high and low frequency alarm level selectors located on the front panel provide a selection of eleven positions including an off position. These alarm level selector switches control voltage dividers which change the D.C. output biases on the rectifier amplifiers and as a result the required signal amplitudes needed to trip the alarm one shot multivibrators.

An audio amplifier was added to each WIT channel in order to use the system in a listening mode. The audio amplifier has a bandwidth of about 100 Hz to 10 kHz. The total gain range, including the preamplifier, is 40 to 80 dB and is controlled by a gain potentiometer located on the front panel. A phone jack, located on the front panel, is also provided for audio headset listening.

Console Circuits

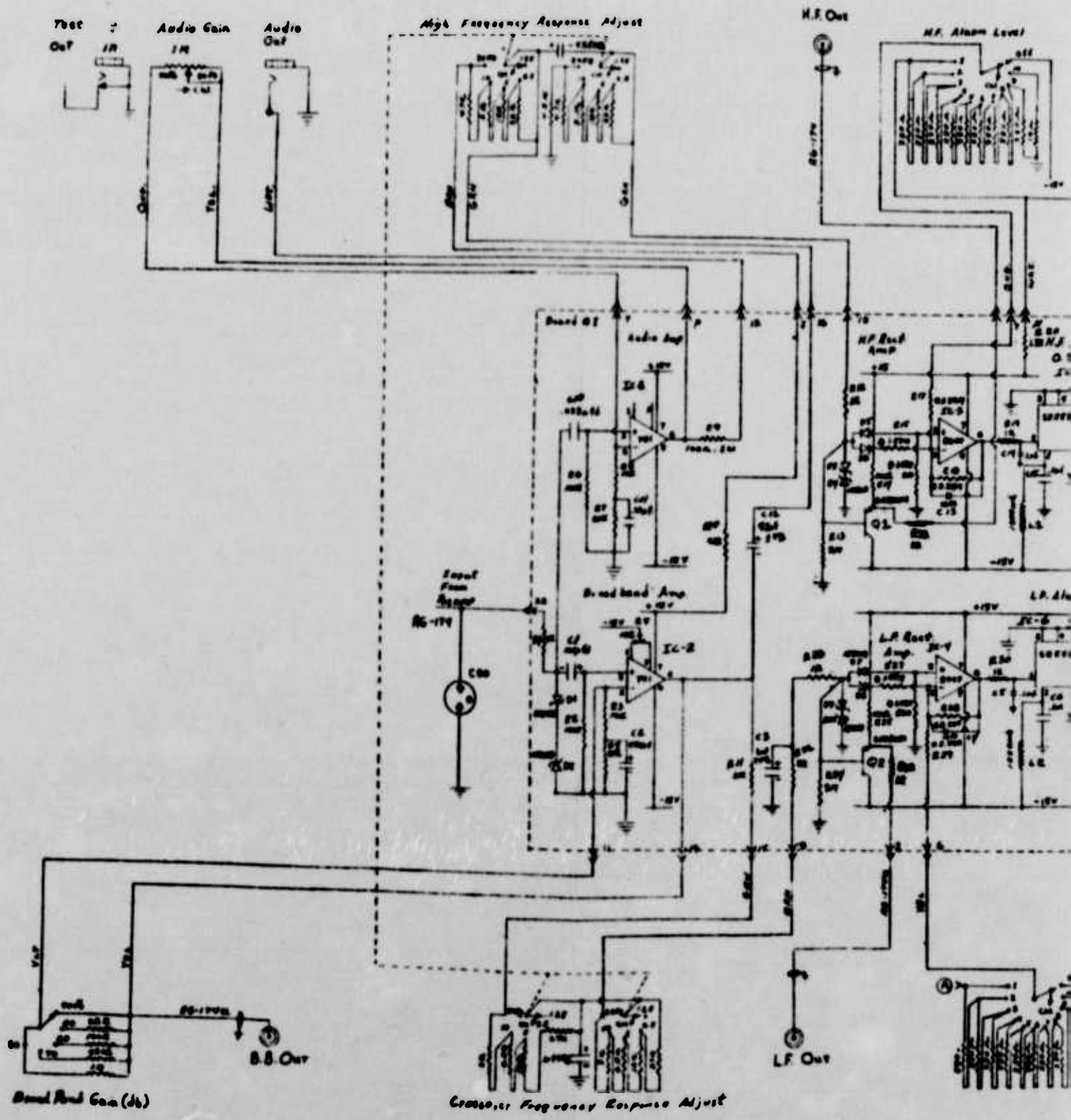
An electronic circuit diagram of the console is shown in Figure A4. There are four identical electronic circuit boards and associated circuits. All of board #1 circuitry is shown enclosed within the dashed lines. The controls are all located on the front panel. Relay and cable connections are located on the rear panel.

The input to each channel is protected with a high voltage Siemens gas arrestor. In addition, Resistor R1 and zener diodes D1 and D2 provide for additional signal amplitude limiting. From here the input signal is coupled through capacitor C1 into the broadband amplifier, which is made up of IC-2 and associated components. Note that the broadband gain switch and associated resistors are part of this amplifier.

The audio amplifier input also takes advantage of the transient signal limiting at the broadband amplifier input. The input signal is coupled through capacitor C10 into the audio amplifier. This amplifier is made up of IC-1 and associated components. The output of the audio amplifier is connected by way of a current limiting resistor R9 to a phone jack.

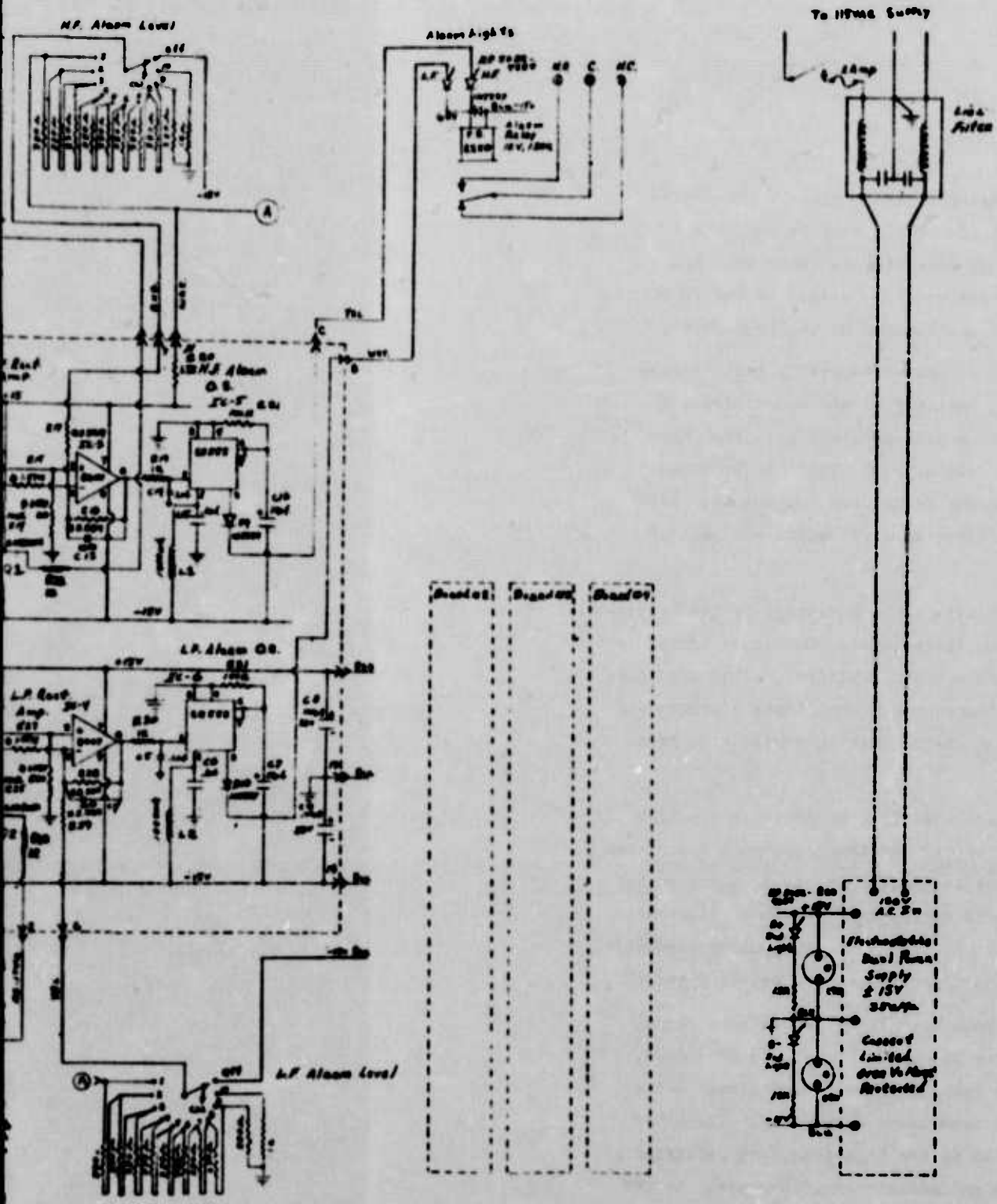
The output of the broadband amplifier connects to the high frequency filter made up of capacitor C12 and the components associated with the high frequency response adjust portion of the selector switch. The broadband amplifier also connects to the low frequency filter made up of resistors R11 and R22, capacitor C3, and the components associated with the low frequency response adjust portion of the selector switch.

The output of the high frequency filter is fed to a signal limiting circuit made up of resistor R12 and zener diodes D3 and D4. One output of the limiting circuit feeds into a emitter follower buffer stage made up of transistor Q2 and associated components. The other limiting circuit output is connected to the high frequency rectifier amplifier which is made up of IC-3 and associated components. At the input to this amplifier are diodes D5 and D6 which split the input



A-8

Figure A4. Schematic Diagram of Console



Console

signal to the two amplifier inputs. Diode D5 permits only negative going input signals to pass, while D6 only permits the passage of positive signals. Since the input to the IC amplifier at pin 3 is noninverting and since the input to pin 2 is inverting, the resulting output at pin 6 appears rectified. Various precision resistors are arranged to provide for the proper bi-polar scaling. The amplifier gain is set at two, which means that a six volt peak to peak signal is fed to the input, the resulting rectified output would be a six volts peak signal.

The high frequency alarm level switch and the associated resistors form a voltage divider network. The switch wiper connects scaling resistor R17 to the divider network providing a positive D.C. bias voltage through R17 to the amplifier inverting input. This results in offsetting the normal zero D.C. output to a negative D.C. output which varies according to the selector switch setting. As a result, when the high frequency alarm level switch is set to position 10, the minimum positive voltage, the signal required to trip the high frequency alarm is maximum since the trip voltage is set at about -10 V. The off position of the selector switch connects a negative 15 V to the rectifier amplifier. This causes the amplifier output to go into positive saturation and even a maximum input signal cannot trip the high frequency alarm.

The output of the high frequency rectifier amplifier feeds into the high frequency alarm one-shot multivibrator. This one shot shown as IC-5 is connected with the positive power bus at ground and the negative bus at -15 V. This establishes the signal voltage trip level at -10 V. The on time of the multivibrator is established by resistor R21 and capacitor C16.

The low frequency rectifier amplifier and alarm one-shot multivibrator circuits are identical in all respects to their high frequency counterparts.

The outputs of the one-shot multivibrators are on pin 10 through blocking diodes D9 and D10. These outputs are connected to high frequency and low frequency alarm lights and then to the alarm relay.

The instrument is powered by a single dual voltage regulated power supply. The positive and negative supplies have a L.E.D. indicator light connected across their outputs. High voltage surge arrestors are also provided across both supplies. The 115 V A.C. power input is provided with a dual line filter to block out power line noise.

U.S. GOVERNMENT PRINTING OFFICE: 1975-614-357/34

*MISSION
of
Rome Air Development Center*

RADC is the principal AFSC organization charged with planning and executing the USAF exploratory and advanced development programs for information sciences, intelligence, command, control and communications technology, products and services oriented to the needs of the USAF. Primary RADC mission areas are communications, electromagnetic guidance and control, surveillance of ground and aerospace objects, intelligence data collection and handling, information system technology, and electronic reliability, maintainability and compatibility. RADC has mission responsibility as assigned by AFSC for demonstration and acquisition of selected subsystems and systems in the intelligence, mapping, charting, command, control and communications areas.



**THIS REPORT HAS BEEN DELIMITED
AND CLEARED FOR PUBLIC RELEASE
UNDER DOD DIRECTIVE 5200.20 AND
NO RESTRICTIONS ARE IMPOSED UPON
ITS USE AND DISCLOSURE.**

DISTRIBUTION STATEMENT A

**APPROVED FOR PUBLIC RELEASE;
DISTRIBUTION UNLIMITED.**